General Disclaimer

One or more of the Following Statements may affect this Document

- This document has been reproduced from the best copy furnished by the organizational source. It is being released in the interest of making available as much information as possible.

- This document may contain data, which exceeds the sheet parameters. It was furnished in this condition by the organizational source and is the best copy available.

- This document may contain tone-on-tone or color graphs, charts and/or pictures, which have been reproduced in black and white.

- This document is paginated as submitted by the original source.

- Portions of this document are not fully legible due to the historical nature of some of the material. However, it is the best reproduction available from the original submission.

Produced by the NASA Center for Aerospace Information (CASI)

NASA Contractor Report 167932

(NASA-CR-167932) MANUAL FOR EXTENDING THE LASER SPECKLEGRAM TECHNIQUE TO STRAIN ANALYSIS OF ROTATING COMPONENTS Final Report (Auburn Univ.) 79 p HC A05/MF A01 CSCL 14B G3/35

N83-15601

Unclas 02431

MANUAL FOR EXTENDING THE LASER SPECKLEGRAM TECHNIQUE TO STRAIN ANALYSIS OF ROTATING COMPONENTS

L.C. Chien, J.L. Turner, John Weathers, and
W.F. Swinson

Auburn University
Auburn, Alabama

November 1982

Prepared for

NATIONAL AERONAUTICS AND SPACE ADMINISTRATION
Lewis Research Center
Under Grant NAG 3-103

TABLE OF CONTENTS

ORIGINAL PAGE IS
OF POOR QUALITY

Introduction

To assist investigators in locating the "critical points" (points of highest magnitudes) in rotating components whole field techniques for strain (or stress) analyses are needed. One such technique is a laser speckle technique that produces Young's fringes. The extension of this speckle technique to the strain (stress) analysis of rotating parts is the object of this paper.

In extending this speckle technique to the analysis of rotating parts use is made of a film plate "sandwich" procedure [1,2]* from which certain advantages are realized. One advantage over point techniques is that the sandwich procedure retains the full field information found in usual specklegrams. An advantage relative to holography is that the information available from specklegrams allows direct evaluation of in-plane displacement which is needed to calculate in-plane stresses [3,4]. An advantage of sandwich specklegrams over usual specklegrams is that the range of measurement can be increased to include displacements on the order of a few microinches up to values approaching 0.1 inch. Also, positive or negative displacement can be assigned to a point using the sandwich speckle procedure, something that usual (single film) specklegrams cannot reveal. Timing constraints for gathering displacement data from a rotating component are considerably relaxed with the sandwich speckle interferometric procedure as compared to holographic and conventional speckle techniques [5,6].

* Numbers in brackets refer to references.

ORIGINAL PAGE IS
OF POOR QUALITY

Finally the analysis of the data for determining strains is more convenient than holographic analyses.

Essentially the speckle procedure involves photographing the speckle produced by a pulsed laser when the laser light impinges on a rotating structural component (or part). In this sandwich procedure the component is then stopped and repositioned as close as one can in the same location that it occupied at the time of the first photograph. A second photograph is then made using the pulsed laser to illuminate the stationary part. The two negatives containing the speckle patterns are sandwiched together with the emulsions in contact and the images realigned relative to each other so that Young's fringes can be observed when a small area of the sandwich is illuminated with a continuous laser. Displacement components can be calculated from the Young's fringe data. Stresses can be calculated by differentiating the displacement data.

Analytical Description of the Sandwich Speckle Fringes:

Consider a point, O, contained in an aperture and illuminated by a coherent light source, S, as illustrated in Fig. 1. The light wave scattered by O to a point P on a distant screen maybe represented by the real part of

$$d\overline{E}_{Po} = \overline{A}e^{i(wt+\phi)}dxdy \qquad (1)$$

$\overline{A}$ = amplitude of the optical disturbance,
w = transverse frequency of light, and
ϕ = phase angle of the optical disturbance.

Let point Q be a nearby point located relative to O by vector $\overline{B}$ where

$$\overline{B} = x\overline{i} + y\overline{j} + z\overline{k} \qquad (2)$$

ORIGINAL PAGE IS
OF POOR QUALITY

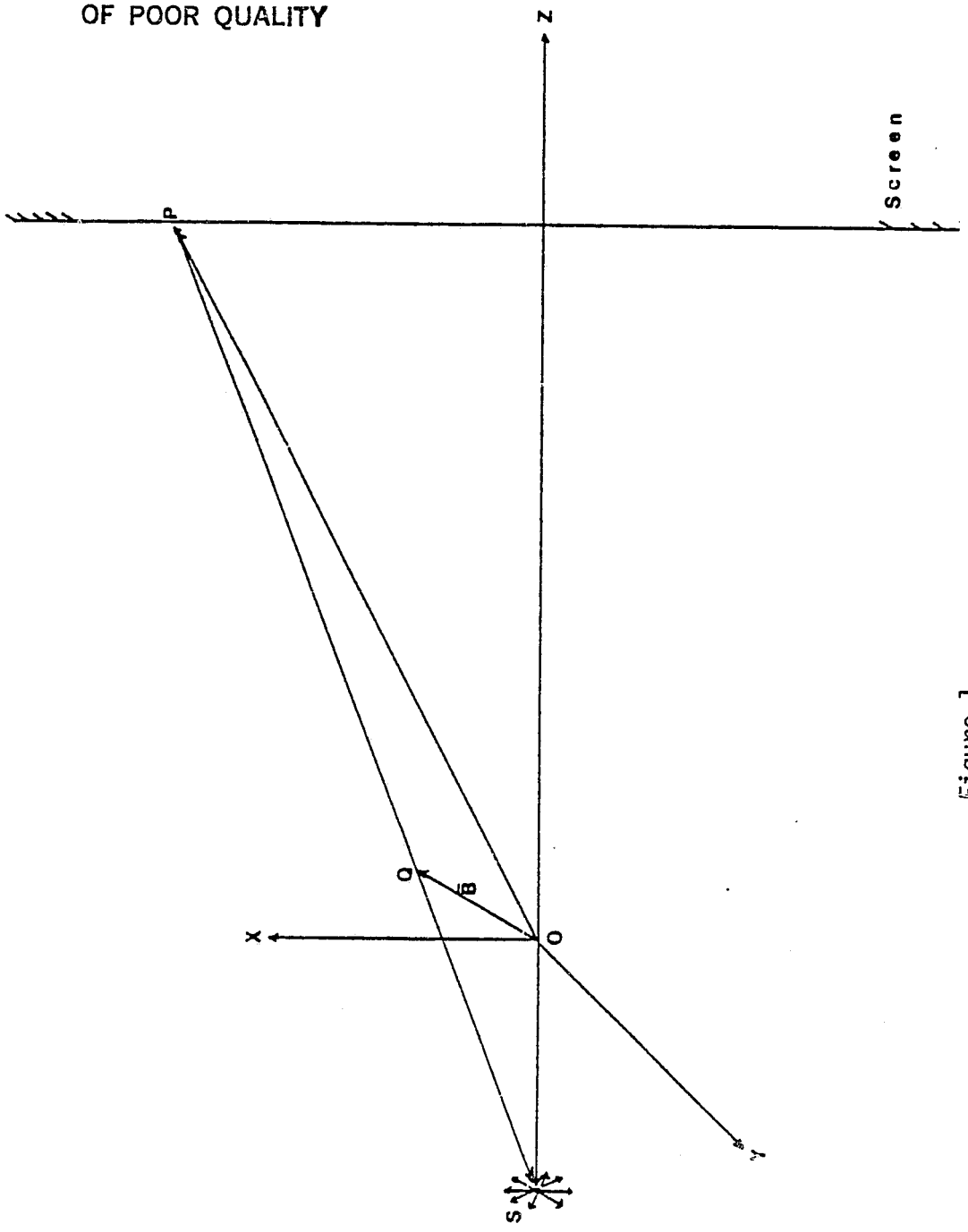

Figure 1

Optic Disturbance

ORIGINAL PAGE IS
OF POOR QUALITY

The optical disturbances O and Q are out of phase by $\Delta\phi$ at point P. The phase difference, $\Delta\phi$, is proportional to the difference in path lengths along $\overline{SOP}$ and $\overline{SQP}$ and is represented as

$$\Delta\phi = \frac{2\pi}{\lambda}\left[(\overline{QS}\cdot\overline{QS})^{1/2} + (\overline{QP}\cdot\overline{QP})^{1/2} - (\overline{OS}\cdot\overline{OS})^{1/2} - (\overline{OP}\cdot\overline{OP})^{1/2}\right] \quad (3)$$

where

λ = the wave length of the coherent light source.

It is noted that

$$\overline{QS} = \overline{OS} - \overline{B} \text{ and} \quad (4)$$

$$\overline{QP} = \overline{OP} - \overline{B} \quad (5)$$

By substituting Eqs. (4) and (5) into Eq. (3), using a bionomial expansion and neglecting higher order terms (assuming $|\overline{B}| << |\overline{OP}|, |\overline{OS}|$) we obtain

$$\Delta\phi = -\frac{2\pi}{\lambda}\left[\frac{\overline{OS}}{(\overline{OS}\cdot\overline{OS})^{1/2}} + \frac{\overline{OP}}{(\overline{OP}\cdot\overline{OP})^{1/2}}\right]\cdot\overline{B} \quad (6)$$

taking

$$\overline{n}_s = \text{a unit vector along } \overline{OS} = -\overline{k} \quad (7)$$

and

$$\overline{n}_o = \text{a unit vector along } \overline{OP} = \ell\overline{i} + m\overline{j} + n\overline{k} \quad (8)$$

then

$$\Delta\phi = -\frac{2\pi}{\lambda}(n_s + n_o)\cdot\overline{B} \quad (9)$$

or

$$\Delta\phi = -\frac{2\pi}{\lambda}[x\ell + ym + z(n-1)] \quad (10)$$

where ℓ, m, n are direction cosines of $\overline{n}_o$. The optical disturbance at P due to Q is now expressed as

$$d\overline{E}_{PQ} = \overline{A}e^{i}\left\{wt + \phi - \frac{2\pi}{\lambda}[x\ell + ym + z(n-1)]\right\}dxdy \quad (11)$$

The combined optical disturbance at P from all points in a two dimensional aperture is

ORIGINAL PAGE IS
OF POOR QUALITY

$$\bar{E} = \bar{A}e^{i(wt+\phi)} \iint e^{-i\frac{2\pi}{\lambda}[x\ell + my + z(n-1)]}dxdy \qquad (12)$$

Consider a small aperture (say aperture 1) centered at the origin and contained in the X - Y Plane. The disturbance at P due to aperture 1 is

$$\bar{E}_1 = \bar{A}e^{i(wt+\phi)} \int_{area} e^{-i\frac{2\pi}{\lambda}[x\ell + ym]}dxdy \qquad (13)$$

Next consider a second aperture the same size as aperture 1 displaced relative to the first by Δx, Δy, Δz. The disturbance at P due to this aperture is

$$\bar{E}_2 = \bar{A}e^{i(wt+\phi)} \int_{area} e^{-i\frac{2\pi}{\lambda}[(x+\Delta x)\ell + (y+\Delta y)\, m + (n-1)\Delta z]}dxdy \qquad (14)$$

or since Δx, Δy, Δz are constants

$$\bar{E}_2 = \bar{E}_1 e^{-i\frac{2\pi}{\lambda}[\Delta x\ell + \Delta ym + \Delta z(n-1)]} \qquad (15)$$

The total disturbance at P then is

$$\bar{E}_{TOTAL} = \bar{E}_1\left\{1 + e^{-i\frac{2\pi}{\lambda}[\Delta x\ell + \Delta ym + \Delta z(n-1)]}\right\} \qquad (16)$$

The intensity at P is given by

$$I_P = C\,\bar{E}_{TOTAL} \cdot \bar{E}^*_{TOTAL} \qquad (17)$$

where

C = proportionality constant

$\bar{E}^*_{TOTAL}$ = complex conjugate of $\bar{E}_{TOTAL}$

Expanding Eq. 17 and collecting terms yields

$$I_P = 2I_1\left\{1 + \cos\frac{2\pi}{\lambda}[\ell\Delta x + m\Delta y + (n-1)\Delta z]\right\} \qquad (18)$$

where I_1 is the intensity due to a single aperture and typically represents a halo while the terms in parentheses represents "Youngs fringes"

ORIGINAL PAGE IS
OF POOR QUALITY

across the halo.

For further consideration of the sandwich technique let the X-axis be coincident with the displacement component being measured (normal to the camera axis) and let Δz represent the "gap" between film plates along the line of sight of the camera.

Then

$$I_p = 2I_1 \left\{ 1 + \cos \frac{2\pi}{\lambda} \left[\ell \Delta x + (n - 1)\Delta z \right] \right\} \tag{19}$$

Fringes occur when

$$\ell \Delta x + (n-1)\Delta z = \frac{N\lambda}{2} \tag{20}$$

with $N = \pm 1, \pm 3, - - -$

If $\Delta z = 0$ or if $\Delta x >> \Delta z$ then Eq. 20 reduces to

$$\Delta x = \frac{N\lambda}{2\ell} \tag{21}$$

or

$$\Delta x = \frac{N\lambda (x^2 + z^2)^{1/2}}{2 \quad x} \tag{22}$$

and is equivalent to the usual double exposed specklegram on a single film plate (Fig 2).

If $\Delta x = 0$, Eq. 20 reduces to

$$(n-1)\Delta z = \frac{N \lambda}{2} \tag{23}$$

which describes a fringe pattern of concentric circles (Fig 3). The spacing between these circles is inversely proportional to Δz.

If Δx and Δz are comparable in magnitude, the resulting fringe pattern is curved (Fig 4).

Data can be interpreted according to Eqs. (20), (22) or (23). If the fringes are relatively straight Eq. (22) yields the desired informa-

ORIGINAL PAGE IS
OF POOR QUALITY

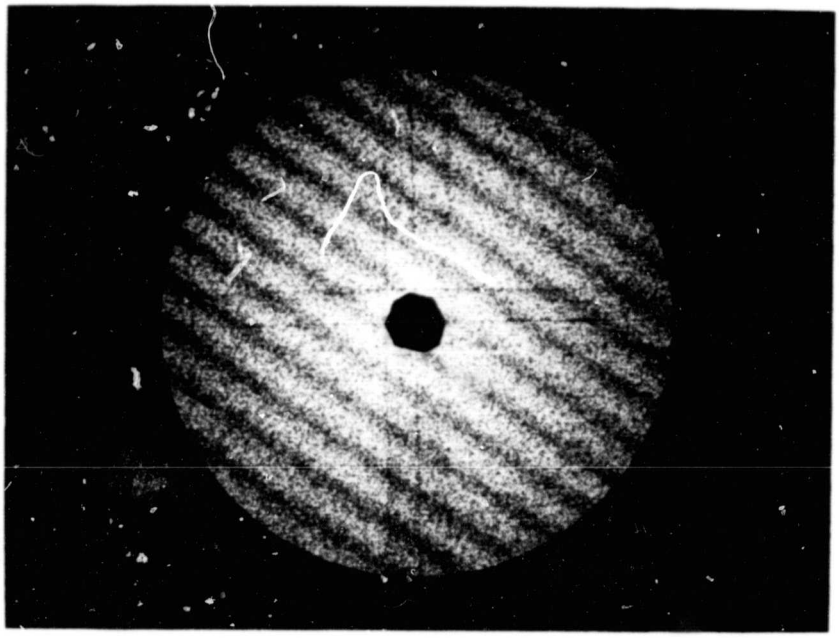

Figure 2. Interference Pattern From Displaced Speckle Patterns

ORIGINAL PAGE IS
OF POOR QUALITY

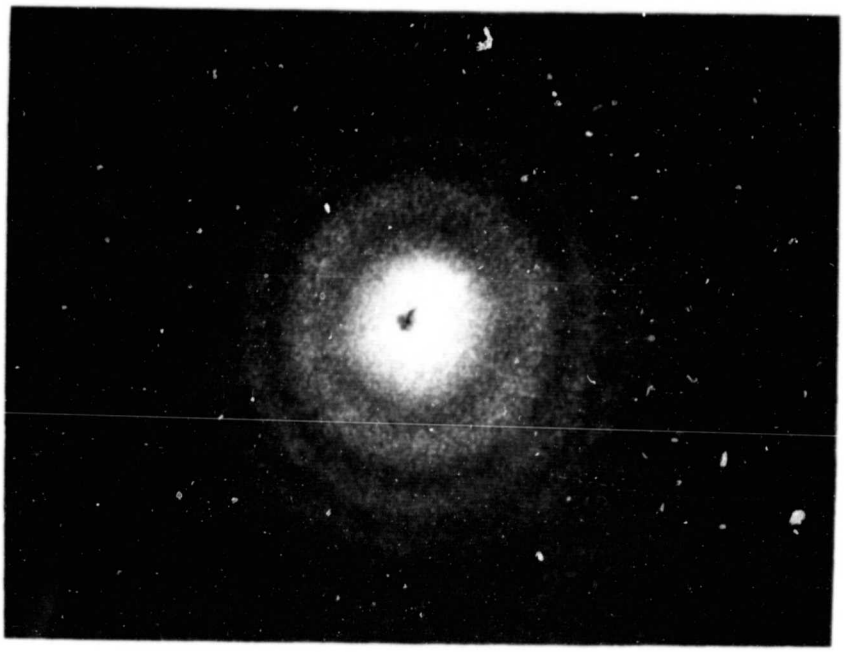

Figure 3. Interference Pattern From Separated Speckle Patterns

ORIGINAL PAGE IS
OF POOR QUALITY

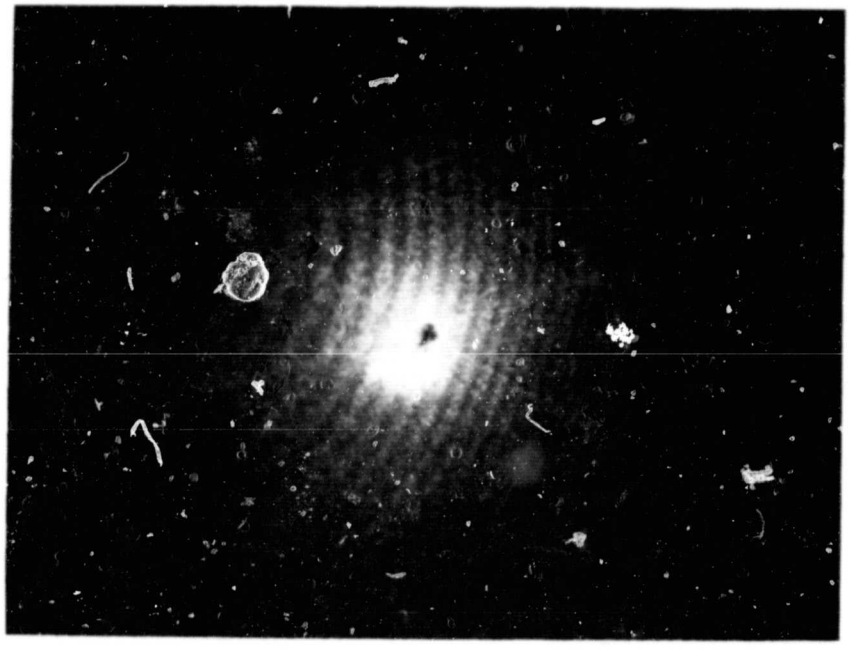

Figure 4. Interference Pattern From Displaced and Separated Speckle Patterns

ORIGINAL PAGE IS
OF POOR QUALITY

tion. If the curvature of the fringes is judged to be significant, translate and/or rotate one speckle photograph with respect to the other until the fringes become concentric circles and evaluate Δz from the concentric rings and Eq. (23). It is noted that $n = z/(x^2 + z^2)^{1/2}$.

Now with the determined value of Δz and Eq. (20) Δx can be evaluated. Alternatively, if the curvature is significant, translate the plates to produce closely spaced Youngs fringes then measure the fringe spacing between adjacent fringes at the center of the halo where (n-1) stays approximately zero. Hence Δz need not be determined explicitly. By letting the second specklegram (the one furthest away from the light source) correspond to a particular specklegram, say the one of the loaded model, more information is available. In this case Δz is positive. Note that "ℓ", (which is X/R) is positive on the positive side of the X axis and negative on the negative side of the X axis, which means that fringes are positive on the positive side of the X-axis and negative on the negative side of the X-axis (see Fig. 5a). Fig 5(c) represents a typical curved fringe pattern. Figs. 5(a) and 5(b) illustrate that the resulting pattern Fig. 5(c) is composed of two parts. One part represented by Fig. 5(a) is due to a displacement along the x axis. The other part (Fig. 5(b)) is due to a seperation of corresponding speckles (or a seperation of the two emulsion film plates.) When part (a) is added to part (b) a curved fringe pattern results as shown in part (c) and indicates that the displacement is toward the center of curvature of the fringes. Part (d) illustrates a negative displacement and when added to the concentric circles of (e) caused by a positive Δz results in curved fringes illustrated in (f). Again note that the displacement

ORIGINAL PAGE IS
OF POOR QUALITY

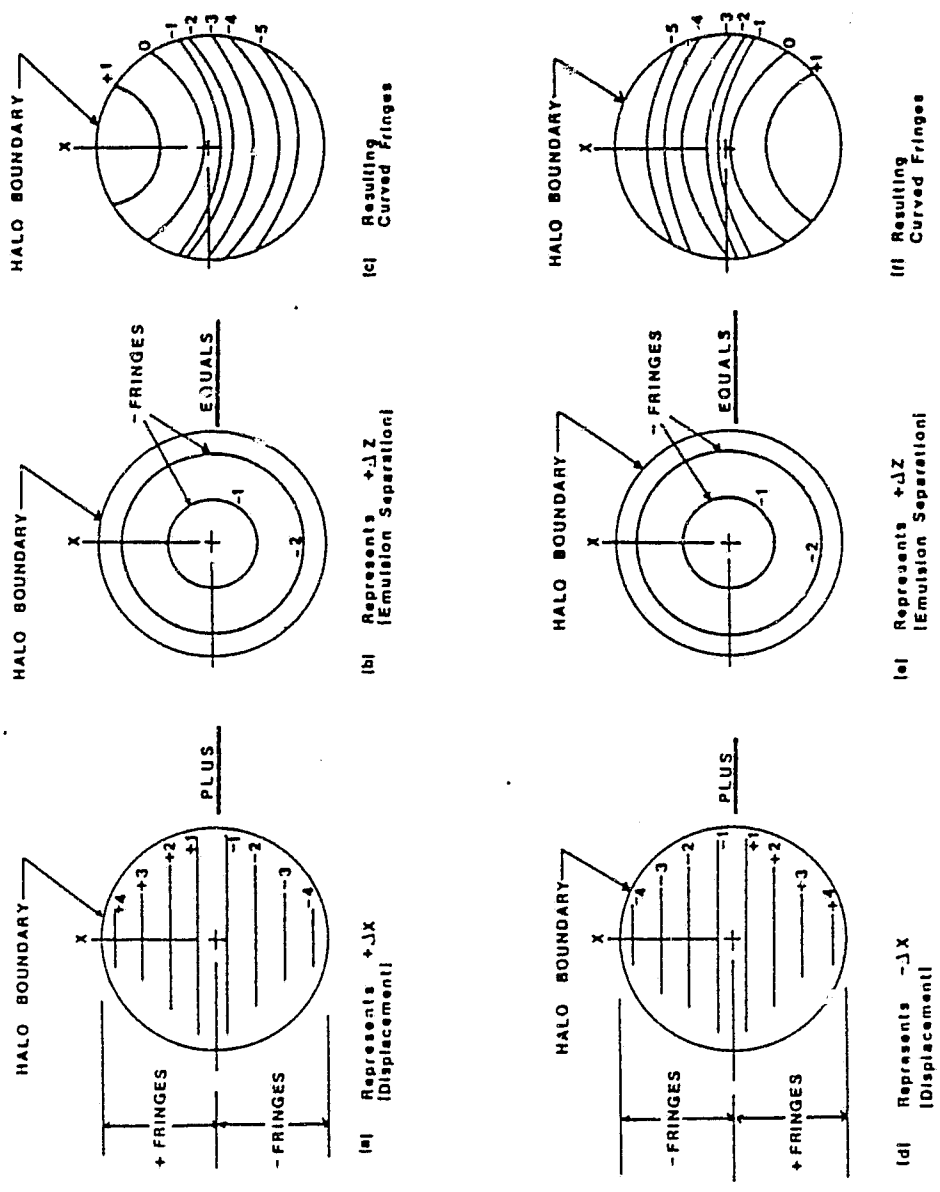

Figure 5

Interference Pattern Illustration

ORIGINAL PAGE IS
OF POOR QUALITY

is towards the center of curvature. Therefore, it is evident that curved fringes can be used to indicate the sign of the displacements. If a fringe pattern is not curved when using the sandwich technique and the positive or negative nature of the displacement at a point is needed Δz can be induced to reveal this information.

Next there are cases when displacements are too small to cause fringes in a halo. For example in a cantilever beam the displacement near the fixed end is small and no Youngs fringes will be evident in the halo circle. In this case the region near the fixed end is the region containing the highest strains and is thus the most important region from a design view point. This difficulty can be alieviated with application of the sandwich technique by mechanically displacing one film plate relative to the other to produce more closely spaced Youngs fringes. The additional fringes correspond to an apparent rigid body movement and do not contribute to the calculated strain components. Normal strain components are expected to be more accurately evaluated than shear strains since rigid body rotations do alter the values of the cross derivatives of displacements. Therefore to evaluate the strain state at a point, it is recommended that the normal strain be determined in three directions, say 0^{o}, 45^{o}, 90^{o}, and these values used to calculate shear strain as is done with strain gage rosette calculations.

Experimental Data Collection:

To explain how data for rotating structural members can be collected via the sandwich speckle technique an example problem is presented.

The example problem selected was made up of two rotating tensile bars with weights on the free end of each specimen for load and balance, Fig. 6 . However, of more importance theoretical strain results could be

ORIGINAL PAGE IS
OF POOR QUALITY

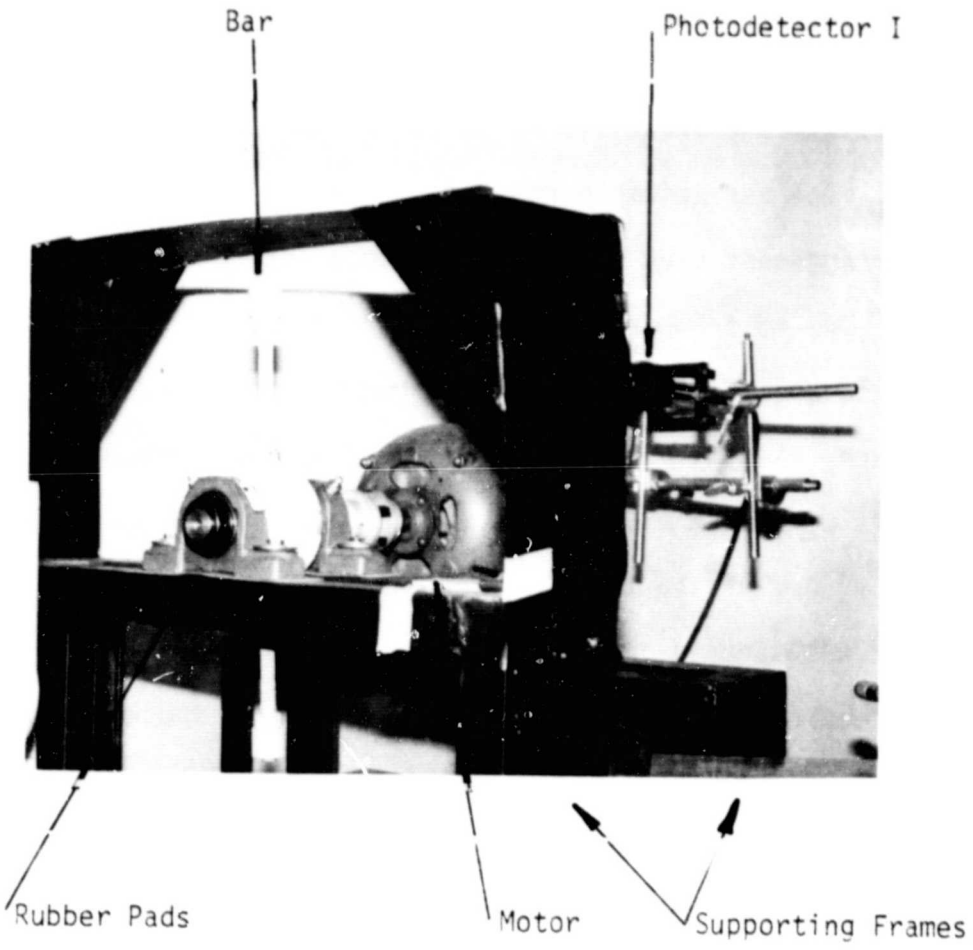

Figure 6. Rotating Bars

ORIGINAL PAGE IS
OF POOR QUALITY

compared with experimental results for evaluation of this experimental technique. Some effort was expended to isolate the system from vibrations by using rubber pads and mounting the rotor shaft in air bearings. It should be emphasized, however, that the speckle technique does not require the same stringent vibration isolation as does holographic techniques. The bar assembly rotated at about 3450 rpm.

The arrangement used to time the events for obtaining data is shown in Fig. 7. The most important component in this arrangement was the pulse ruby laser. First it produced coherent light necessary for a speckle photograph. Secondly by being pulsed a dynamic event could be recorded on film without blur. Data was gathered by taking a speckle photograph of one of the tensile bars while it was rotating. Next the tensile bar was stopped and repositioned in the same location that it had when the dynamic photograph was recorded and a speckle photograph taken. The two negatives were sandwiched together and adjusted relative to each other until Young's fringes could be seen as a laser light was passed through a small area of the negative. When Young's fringes could be seen the negatives were judged to be correlated.

The sequence of events for making the specklegrams is noted. The motor for rotating the tensile bars was turned on and ran for several minutes to obtain a stable rotation. The timing sequence for the dynamic specklegram was initiated by pressing the single beam reset lever of oscilloscope I. One of the tensile bars had a small mirror glued to it. When the mirror reflected the CW argon laser beam (after reset) on to photodetector I an electrical pulse initiated a timing signal for A-gate (a 20 volt pulse) of oscilloscope I. The timing signal was set

ORIGINAL PAGE IS
OF POOR QUALITY

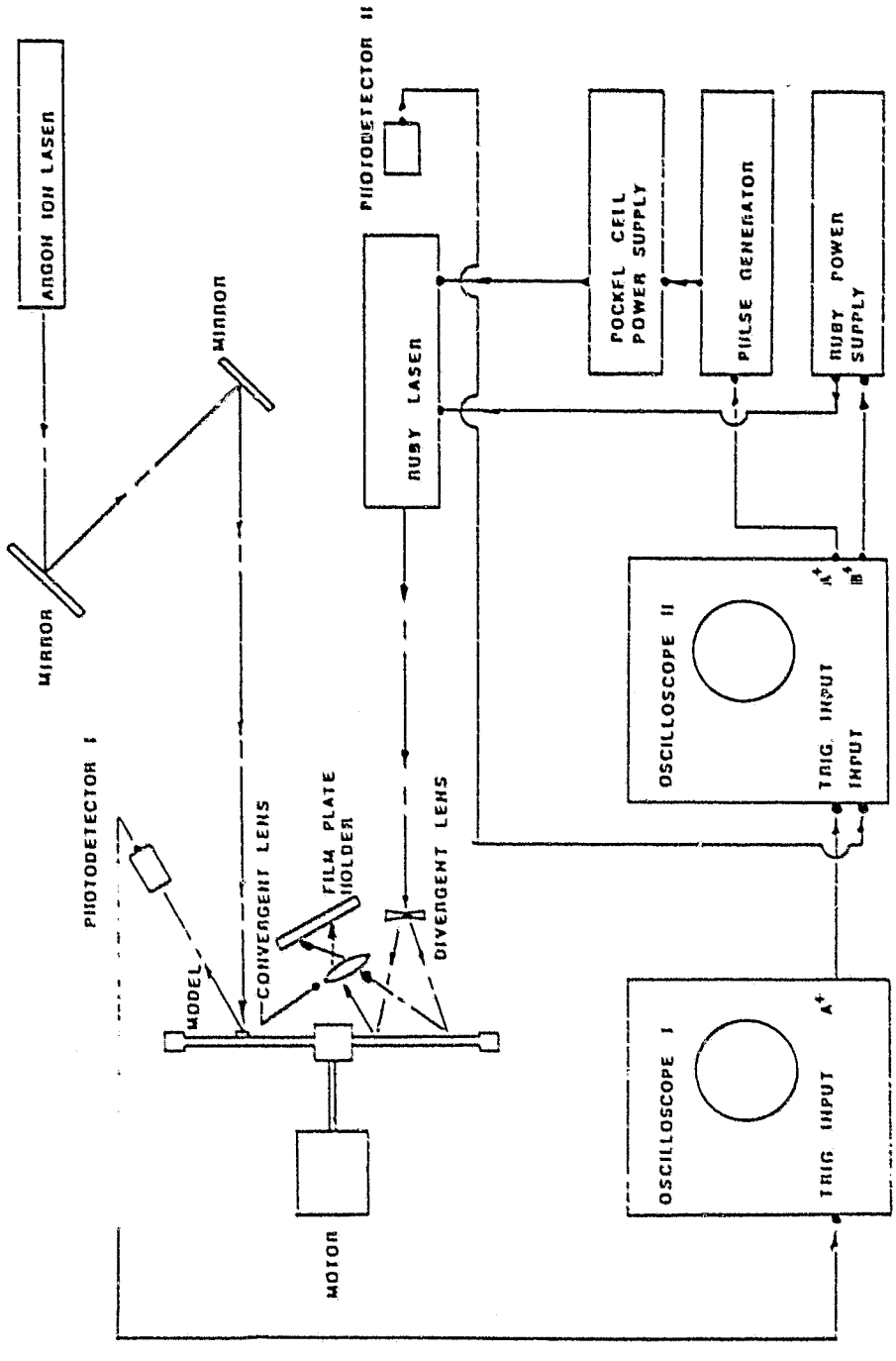

Figure 7

Schematic of Events

ORIGINAL PAGE IS
OF POOR QUALITY

so that the desired tensile bar would rotate into proper position as the ruby laser pulsed to make a specklegram. Time (between 1.0 and 1.5 milliseconds) had to be allowed for the ruby laser power supply to energize the ruby laser. During this interval between 1.0 and 1.5 milliseconds the pulse ruby laser was Q-switched and the ruby laser delivered a large burst of light for about 50 nonoseconds duration. The sequence occured as follows. The timed 20 volt signal (A-gate) from oscilloscope I triggered oscilloscope II. At this instant B-gate (20 volt pulse) of oscilloscope II turned on the ruby laser power supply. One millisecond after B-gate activated the ruby power supply, A-gate of oscilloscope II triggered the pockel cell pulse generator. The pockel cell pulse generator sent a 100 volt switching signal (1.5 microseconds in duration) to the pockel cell power supply. The pockel cell was switched off and then on, allowing the ruby laser to pulse. The coherent pulsed laser illuminated the rotating tensile bar and a dynamic specklegram was recorded. The dynamic specklegram film plate was positioned with the emulsion toward the camera lens and directly against a blank glass plate of equal thickness. The blank glass plate was used so that the light path of the dynamic specklegram would approximate the light path of the second (or stationary) specklegram, where the emulsion is faced away from the camera with the glass film backing in between. These steps made it possible for the two emulsions from the specklegrams to be placed in direct contact during the sandwich process. After developing and drying the dynamic specklegram, it and the glass blank were repositioned in the film holder. The film holder is shown in Fig. 8. The screws located the surface of the glass blank that was closest to the camera lens. The glass, in turn located

ORIGINAL PAGE IS
OF POOR QUALITY

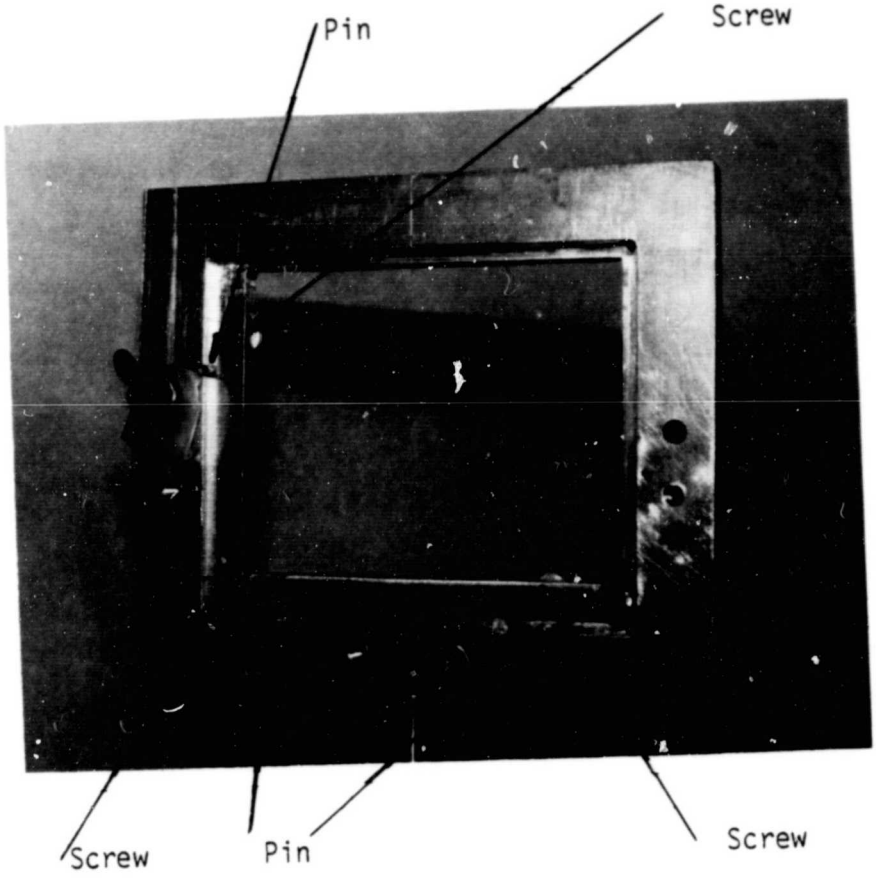

Figure 8. Film Holder

ORIGINAL PAGE IS
OF POOR QUALITY

the film emulsion plane. The pins positioned the glass blank and the film edges. The rotating bar which was photographed in the dynamic specklegram was repositioned in the same imaged location by viewing through the repositioned film. With the bar in this imaged position the glass blank and dynamic specklegram were removed from the holder. Now a stationary specklegram was taken of the stationary bar by light scattering from the bar, through the lens, through the film glass backing and activating the emulsion. This procedure as noted before made it possible to sandwich the two specklegrams (the dynamic and stationary specklegrams) together with the emulsions touching. It should be noted that there was no opaque backing on the film glass of the stationary specklegram so that the pulsed light could pass through the glass backing and activate the emulsion.

Next in the sequence after developing and drying the stationary specklegram, the dynamic and stationary specklegrams were sandwiched together and held with the positioner shown in Fig. 9. This positioner holds one film fixed while the second film is translated and/or rotated relative to the first such that Young's fringes could be observed. During this trial and error process if Young's fringes are observed the negatives are optically correlated such that the wave front generated through the first negative interferes with the wave front generated through the second negative. A typical fringe pattern is seen in Fig. 10. When fringes were observed the two films were locked together and data was taken at the desired points using the scheme shown in Fig. 11. In this illustration with the film emulsions together the spacing, ΔZ, between the emulsions occured only due to slight variation in flat-

ORIGINAL PAGE IS
OF POOR QUALITY

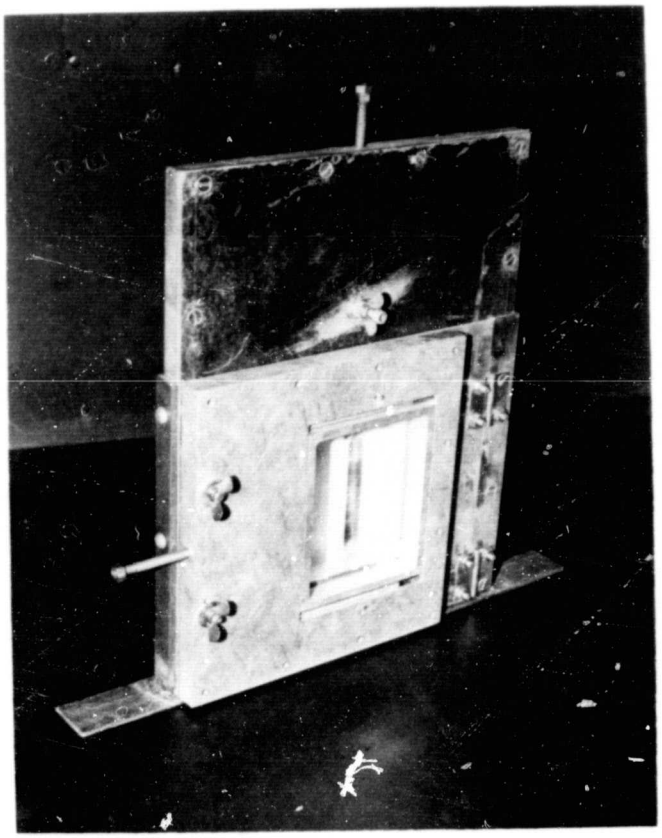

Figure 9. Film Positioner
(A)

ORIGINAL PAGE IS
OF POOR QUALITY

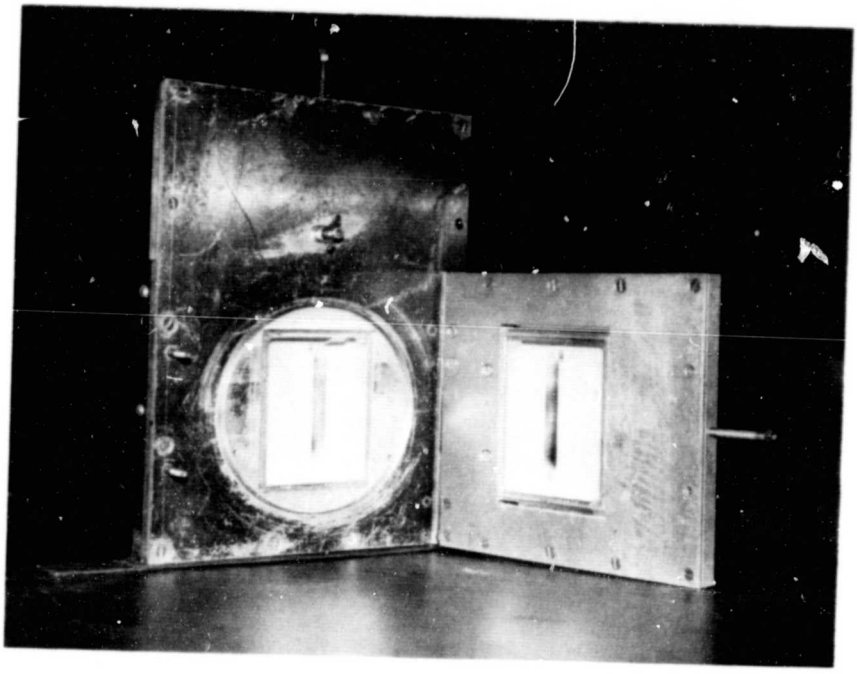

Figure 9. Film Positioner
(B)

ORIGINAL PAGE IS
OF POOR QUALITY

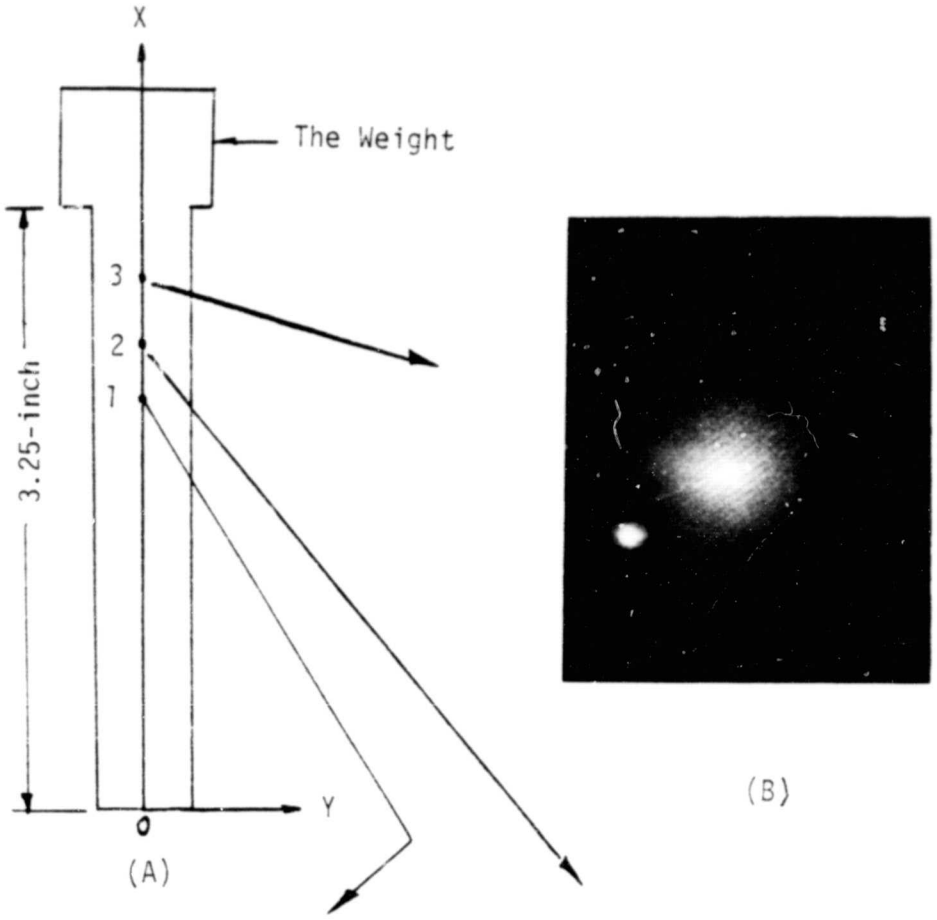

(B)

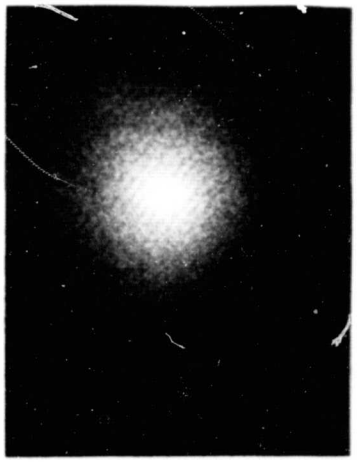

(C)

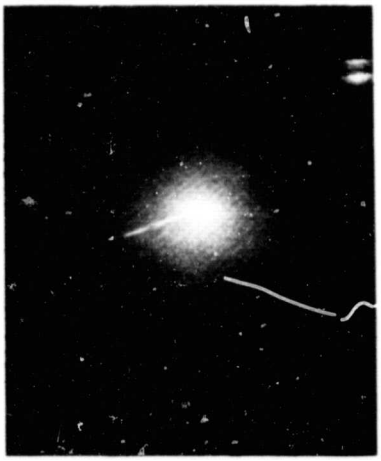

(D)

Figure 10. Interference Patterns From Rotating Bars

ORIGINAL PAGE IS
OF POOR QUALITY

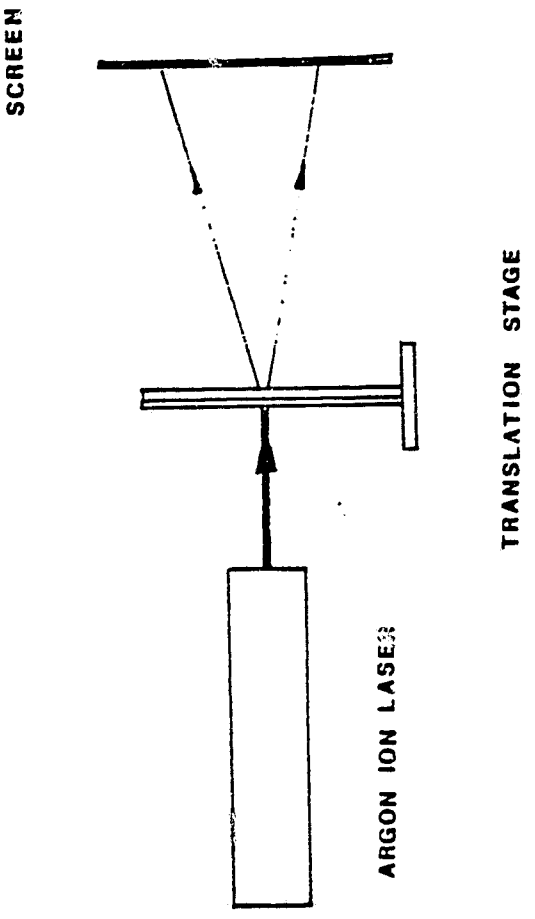

Figure 11

Data Collection

ness of the film plates. The amount of variation, ΔZ, was not needed in the calculations and was not determined. Sometimes the dynamic and stationary specklegrams would not correlate. In these instances the specimen (bar) position was rotated slightly (say 4 or 5 thousandths of an inch at the bar tip) and a second stationary specklegram recorded. If the dynamic specklegram and the second stationary specklegram would still not correlate a third stationary specklegram was taken in the other direction relative to the original position. Two to three trials usually produced correlation. It was noted that in a controlled experiment with a continuous laser as much as 0.07 inch shift between specklegrams was possible without loss of correlation.

Strains were calculated at various points on the centrifugally loaded bar and compared with theoretical values. In this example, calculations were simplified since displacements at the center of the bar were axial. Thus it was only necessary to find the displacement values at these points and to numerically differentiate to obtain axial strains. A second order central difference formula was used to evaluate the derivatives. We chose the data points to be 0.0625 inch to each side of the point of interest. The theoretical calculations were made assuming no significant bending and treating each cross section to be in uniform tension. The tension was calculated using the inertia vector caused by the material mass from the point of interest radially outward. Results of three example points are tabulated in Table I.

Table I. Experimental Results

Point	Distance from centerline to interest point, inches	Calculated strains from data in/in	Calculated strains from theory in/in	%Difference Based on Experiment
1	2.125	305×10^{-6}	295×10^{-6}	3.3
2	2.417	289×10^{-6}	293×10^{-6}	1.4
3	2.750	274×10^{-6}	288×10^{-6}	5.1

The results seem to compliment each other and suggest the credibility of this approach for analyzing strains (or stresses) in rotating parts.

Stresses which are induced in structures because of the rotation of the structure can be evaluated with speckle techniques. The data in comparison with holography data is easy to obtain and especially easy to analyze. Motion or vibration of the structure is not as restricted with speckle techniques as with holographic techniques. The data collected is essentially full field.

The following paragraphs deal with numerical techniques for interpreting laser speckle data.

Integration of Laser Speckle and
Finite Element Techniques of Stress Analysis:

Contemporary methods of stress analysis for design of complex structural components generally fall into two categories: (1) Experimental methods, (2) Numerical techniques. Examples of current experimental methods include laser related techniques (holography, speckle interferometry), grid methods (Moire analysis) and photoelasticity. Some of the currently used numerical techniques include finite element modeling, finite difference analysis and numerical boundary integral methods. Both types of approaches exhibit distinct strengths and weaknesses. For example, the experimental methods of holography and speckle interferometry yield measurements of surface displacements of a structure. The determination of stress typically requires differentiation of this data and can result in a substantial loss of accuracy. Also regions of maximum stress are sometimes regions of relatively little displacement; thus, experimental data may be sparce in those areas. Numerical analysis (eg. finite element modeling) however, is often capable of accurate stress evaluation but requires an accurate knowledge of boundary conditions (boundary displacements and/or tractions). Such boundary conditions are not always known (eg. surface pressure loads on a rotating turbine blade). The potential exists for combining these techniques in a complimentary fashion to make more effective use of their respective strengths and to overcome their separate limitations. By developing procedures for effectively intermeshing the two types of analysis techniques a potentially more effective tool for stress analysis and structural component design can be expected. Investigation of this possibility constitutes the problem examined herein.

Related Research For Use of Laser Speckle and Numerical Techniques:

Relatively little research has been devoted to developing an integrated approach to stress analysis of the type proposed herein. Traditionally, the experimental and numerical techniques have been used as separate tools with application to a common problem primarily for comparison and validation of results. Occasional reports of the use of experimental data for input to a numerical model have appeared (7,8) but without particular effort toward developing or exploring the potential of this concept. Rowlands (9) reported the use of a finite element type discretization and curve fitting technique on experimentally obtained (Moire) displacement data for strain analysis. His results were encouraging but his method did not fully exploit the strengths of the finite element method in that all model displacements were specified from experimental data. Thus, equilibrium and structure geometry played no role in the strain calculations. Additionally, Rowland's approach requires a large amount of experimental data in the regions of interest. This requirement cannot always be met when using displacement measurement techniques.

Recent reports of the combined use of experimental laser speckle and numerical boundary integral techniques have appeared. (10,11) In this approach a relatively small region of interest on the structure is "isolated" for analysis. Experimental displacement data is collected around the boundary of this region and used as input data to a numerical model of this sub-region. Good results have been reported for the test problems that were investigated. A limitation of this approach is the

inherent constraints on the boundary integral method as a numerical technique. It is best suited to modeling small regions over which gradients do not change appreciably. An entire complex structure cannot be effectively modeled with this technique. Thus regions of critical stress must be known apriori. Again, a large amount of experimental data must be available in the region of interest. Finally, the technique is not easily adapted to handling complex conditions (eg. non-homogeneities or anisotropy) as is the finite element approach. It is noted that the finite element modeling approach can be used in precisely the same manner as the boundary integral method in that sub-regions are easily modeled provided the boundary conditions for the sub-region are available. Finite element modeling is not restricted to sub-region analysis however, and is generally more flexible in its applications than other numerical techniques.

General Description of Speckle Analysis With Finite Elements:

Speckle interferometry is a technique for experimentally measuring "in plane" displacements (displacements normal to the direction of sight) of a loaded object. This technique makes use of the fact that the small imperfections of a surface uniquely "map out" that surface (the imperfections determine a "fingerprint" of the surface). To record the in plane displacements of an object, the characteristic pattern of the surface under consideration is obtained by illuminating the unloaded object with a coherent light source (such as a laser) and photographing the image of the surface. The object is then loaded, producing the displacements, and the photographic film plate is exposed a second time. The film

now has a record of the characteristic pattern of the surface imperfections and a record of how that pattern was distorted when the object was loaded. If a beam of coherent light is passed through a small portion of the processed film plate, the two patterns will cause the light waves to interfere and produce fringes which can be related to the in plane displacement of the illuminated point on the image. This experimental technique is well suited to the study of relatively flat members loaded in a plane stress state although other applications are possible.

Once displacements are obtained, the conventional method of obtaining stresses is to numerically differentiate the displacements at the point of interest to determine strain components and then to use constitutive equations to obtain stresses. This requires displacements to be obtained at many points in the area of interest. Unfortunately, areas of interest (areas of high stresses - large displacement gradients) are not necessarily areas with large displacements. If displacements are below the resolution of the measurement technique, insufficient experimental data is available for local strain determination.

Use of the finite element method allows (if necessary) displacement data to be obtained away from the area of interest and in an area where more accurate data can be collected. The finite element approach to be used with speckle interferometry should accept displacement data to specify the boundary conditions for the area under consideration. Hence, a conventional "displacement" formulation of the finite element model is suitable. The boundary conditions are determined by specifying the displacements surrounding the area of interest, not necessarily close to the points of interest. Additional boundary conditions, such as

stress free surfaces, are also readily accommodated. The finite element method then uses the physical characteristics of the structure along with the experimentally determined boundary conditions to determine the stress distribution throughout the area of interest.

Description of Finite Element Program and Modeling Considerations

A suitable element computer program into which experimentally obtained displacement data can be input has been developed in-house. The program employs a six-node, plane stress triangular element. The element nodal points are located at the verticies and midsides of the triangle. Two orthogonal components of displacement are permitted at each nodal point; thus, twelve displacements or, "degrees of freedom" are associated with each element. The displacement field within each element is interpolated from the nodal displacements through complete, second degree polynomial functions. Thus, linear stress distributions are permitted within each element. All criteria for guaranteeing convergence to the "exact" solution as the element mesh is refined have been met with this element. The program is capable of modeling linear elastic, nonhomogeneous, anisotropic plane stress problems. Thermal stress modeling is also possible. Any combination of nodal point displacement values can be specified. Boundary tractions (normal and shear stresses) can also be specified as well as "point loads".

To facilitate application of the program an automatic grid generation subroutine was developed. By defining model boundary geometry an internal mesh of triangular elements with associated nodal coordinates and connectivity parameters can be automatically generated with this routine. Figure 12 illustrates grid generation for a complex structure

ORIGINAL PAGE IS
OF POOR QUALITY

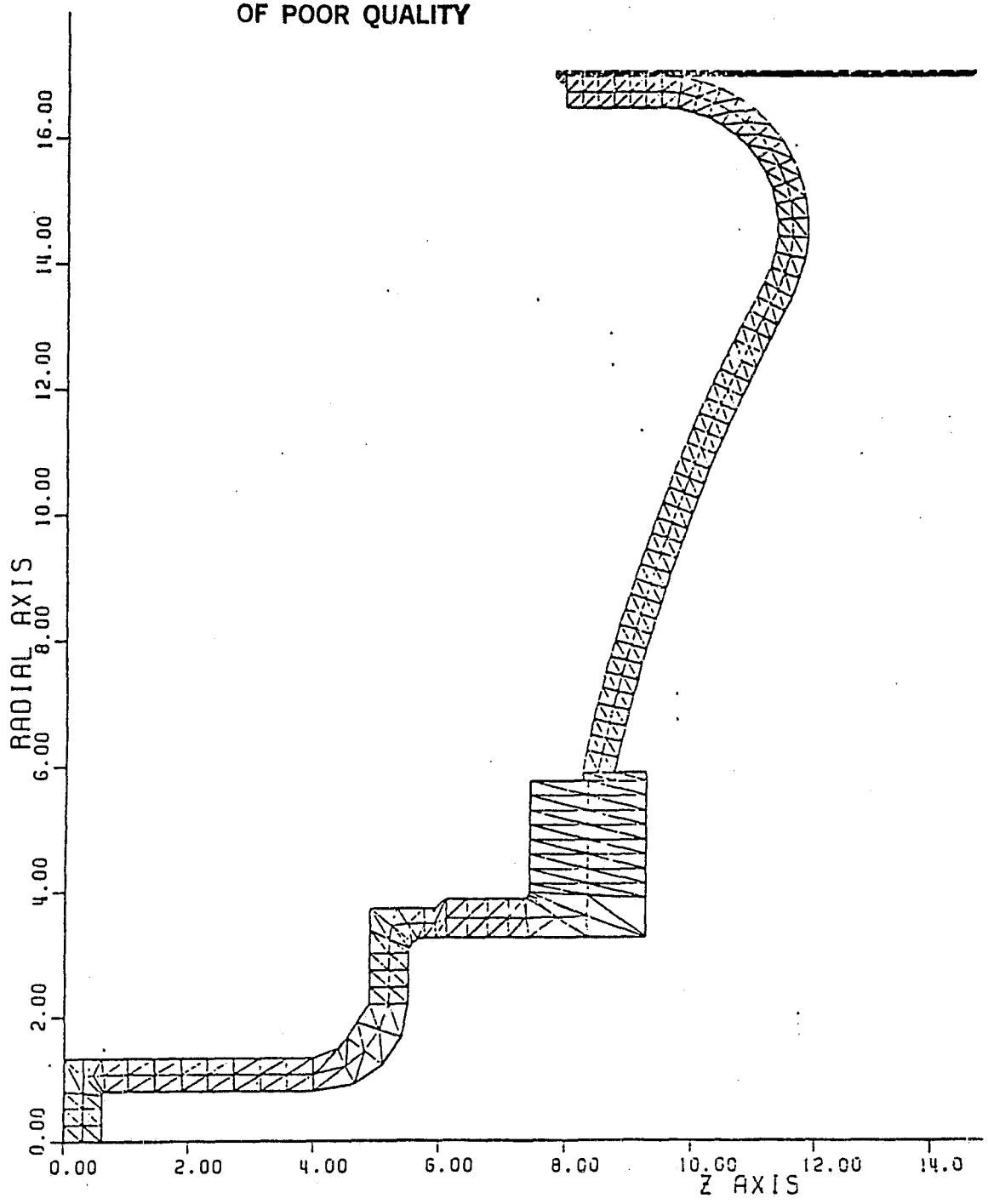

Figure 12

Automatic Grid Generation of a Complex Structure

by use of this program.

This finite element program was validated on several trial problems with known solutions and found to give excellent results. The linear strain triangle is relatively insensitive to aspect ratio and is far superior to a three node, constant strain triangular element. Rigid body movement can accompany the deformation without altering the stress field. This feature is important since experimentally measured displacements usually include some contributions from rigid body movement.

Some judgement is necessary regarding mesh refinement for problems where stress gradients are not known apriori. Consideration of the permitted stress variations across individual elements together with anticipated stress gradients in regions of stress concentration should form the primary guidelines for grid selection.

When analyzing a structure or a sub-region of a structure by finite element analysis, boundary conditions on all defining boundaries of the grid must be specified before the problem can be solved. Either displacements (experimentally determined or otherwise), boundary stresses or combinations of both can be used. The selection should be based on the boundary conditions that are known with the most certainty. If displacements are experimentally measured by laser speckle techniques, for example, it is likely that displacement boundary conditions can be determined along all boundaries. If a portion of the boundary is, however, free of applied traction, this stress boundary condition should be used in lieu of experimental displacement data along that boundary. This is because such a condition can be enforced and be totally free of experimental error. It is noted that most finite element programs are written such that boundaries

are automatically assumed to be "stress free" unless otherwise specified. Thus this type of stress boundary condition usually need not be explicitly specified with input data to the program. Displacements and non-zero boundary tractions are explicitly input as data. It should also be realized that random pertabations in boundary data (perhaps due to experimental error) can significantly affect local stress values. Saint Venant's principle indicates these effects to be localized in some sense provided that the boundary conditions are statically correct overall.

These comments are intended to provide some general guidelines for consideration when selecting boundary conditions from experimental data for use in finite element modeling.

A copy of the finite element program is included in the appendix.

Application of Laser Speckle/Finite Element Technique:

Two applications of the Laser Speckle/Finite Element Technique are presented. The first application is to a cantilevered beam with a constant distributed load applied from the middle to the end of the beam. The second application is to a "C-ring" in diametrical compression.

The Cantilevered Beam:

This example is given to illustrate how the completeness of description of the displacements at the points of applied loads effect the accuracy of the stress distribution obtained. Laser speckle data was not obtained. Instead, displacements were determined analytically from beam theory for an aluminum cantilevered beam 1 inch wide, 15 inches long and 1/4 inch thick with a constant distributed load of 3 lb/in applied from the middle to the end of the beam. For finite element analysis the beam was modeled using 20 plane stress elements, Fig. 13.

Five different cases were analyzed. The first case [Case 1] had the displacement at the end of the beam due to the distributed load as the only input into the F.E. (finite element) program. The other points on the surface had their boundary conditions left to their default values of being stress free (the stress free condition is the most accurately known boundary condition except in areas where a force is known to be applied, such as under the distributed load). Case 2 had the displacements at the start and end of the distributed load input into the F.E. program; Case 3 had displacements input at the start, middle and end of the distributed load; Case 4 had displacements input at six points (every other node) under the distributed load; and Case 5 had the displacements at every node (eleven points) under the distributed load input into the

ORIGINAL PAGE IS
OF POOR QUALITY

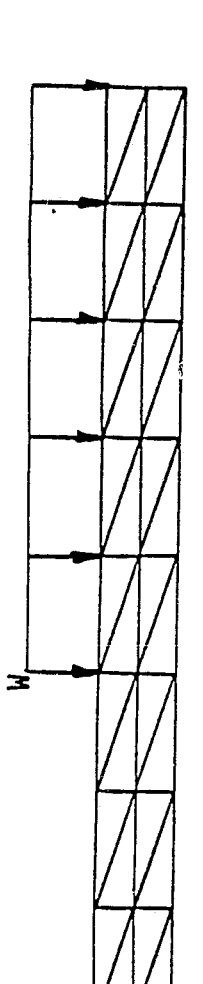

Figure 13. Finite Element Modeled Cantilever Beam

finite element program. The normal stress, σ_X, at the surface versus the length of the beam has been plotted for these five cases and are shown in Figs. 14 - 18 . Note that as the displacements at the applied load were more completely described, σ_X approached the analytical curve for σ_X.

For the second application it was desirable to apply the Laser Speckle/Finite Element Technique to a model in a nontrivial plane stress state. It was also desirable to chose a model for which an analytical solution was known. A "C-ring" in diametrical compression satisfied both of these requirements. The stress state is nontrivial due to the curved beam nature of the model; an analytical solution is available in Theory of Elasticity, by Timoshenko and Goodier.

The C-ring had an inside diameter of 3 inches and an outside diameter of 4 inches. It was made of aluminum and was 1/4" thick.

Equipment was needed to hold the C-ring and to provide reference measurements. In order to load the ring in diametrical compression a special test rig was built, Fig. 19 . This rig allowed displacement along a diameter of the ring by applying a force through a hydraulic cylinder arrangement. One of the main considerations in designing the test rig was to restrain the C-ring from any movement out of the plane of interest without inducing any additional forces which would effect the stress distribution.

In order to measure the diametrical displacement the C-ring experiences, a dial indicator (accurate to 0.0001 inches) was mounted along the diameter through which the force was applied. A calibration specimen was also included in the experimental setup so that an object under-

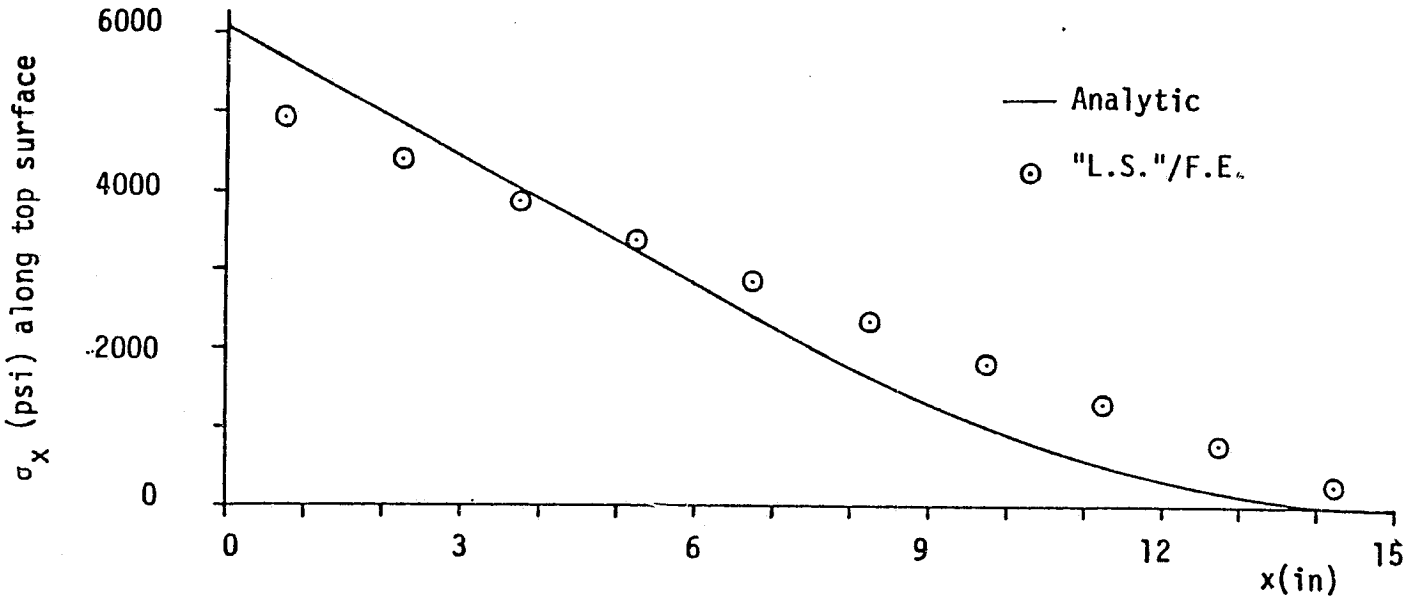

Figure 14. σ_x Along Top Surface Versus End Displacement For Cantilever Beam

ORIGINAL PAGE IS
OF POOR QUALITY

ORIGINAL PAGE IS
OF POOR QUALITY

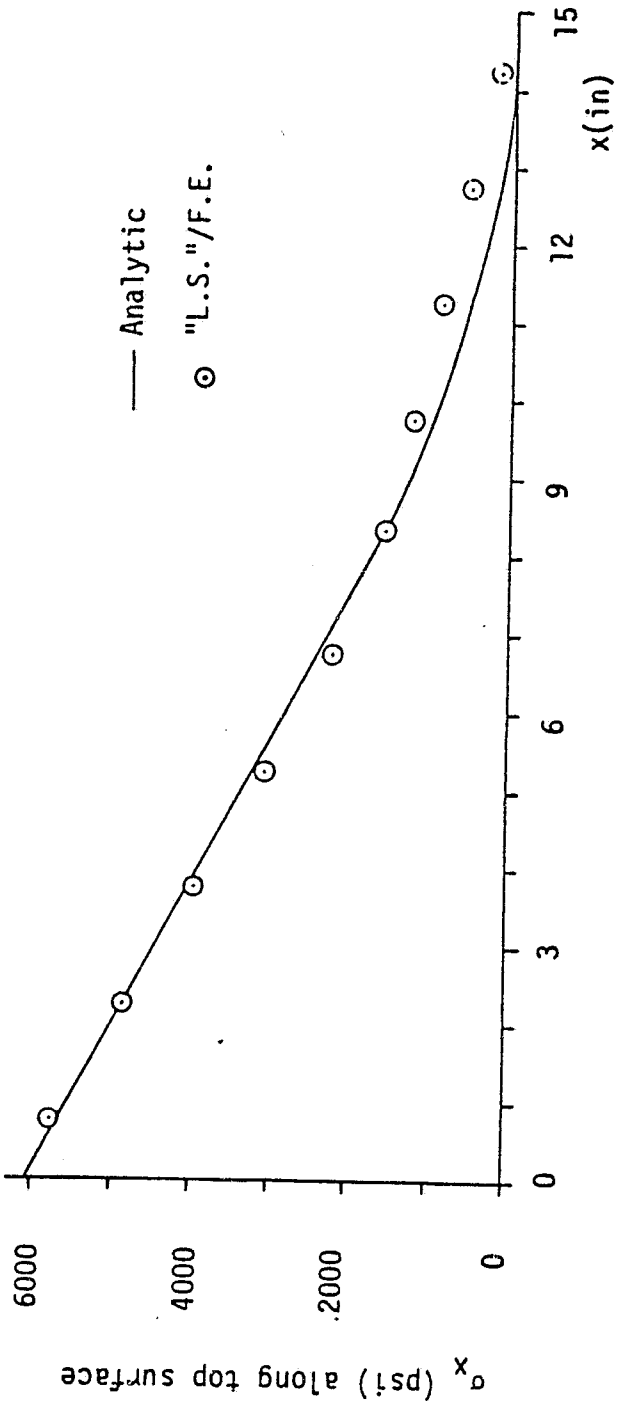

Figure 15. σ_x Along Top Surface Versus Displacement At Start And End of Distributed Load For Cantilever Beam

ORIGINAL PAGE IS
OF POOR QUALITY

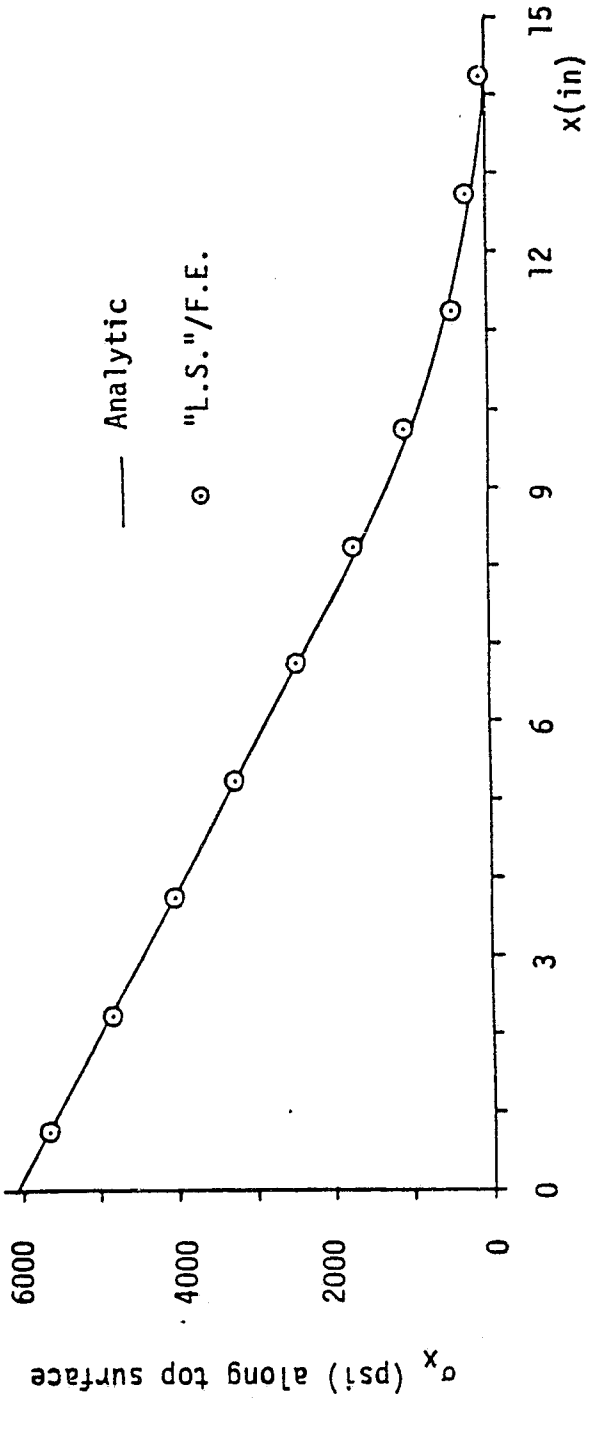

Figure 16. σ_x Along Top Surface Versus Displacement at Start, Middle and End of Distributed Load For Cantilever Beam

ORIGINAL PAGE IS
OF POOR QUALITY

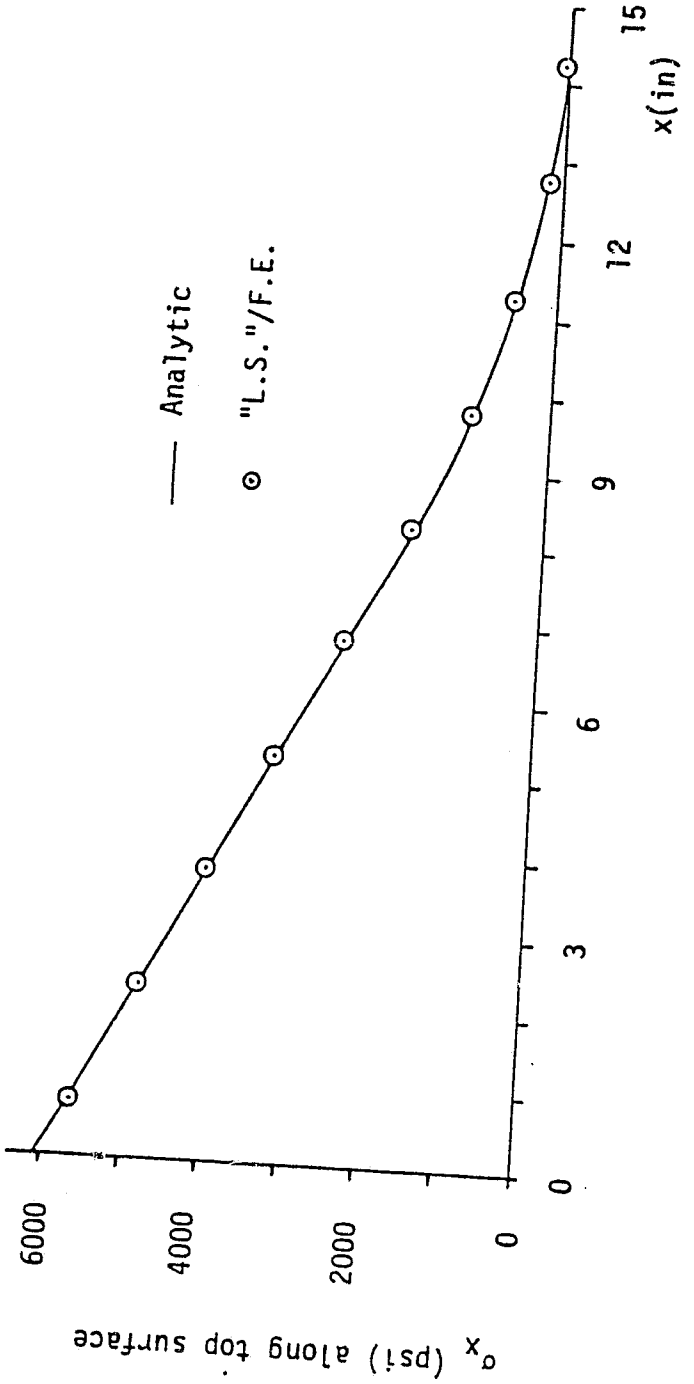

Figure 17. σ_x Along Top Surface Versus Displacement At Every Other Node Under Distributed Load For Cantilever Beams

ORIGINAL PAGE IS
OF POOR QUALITY

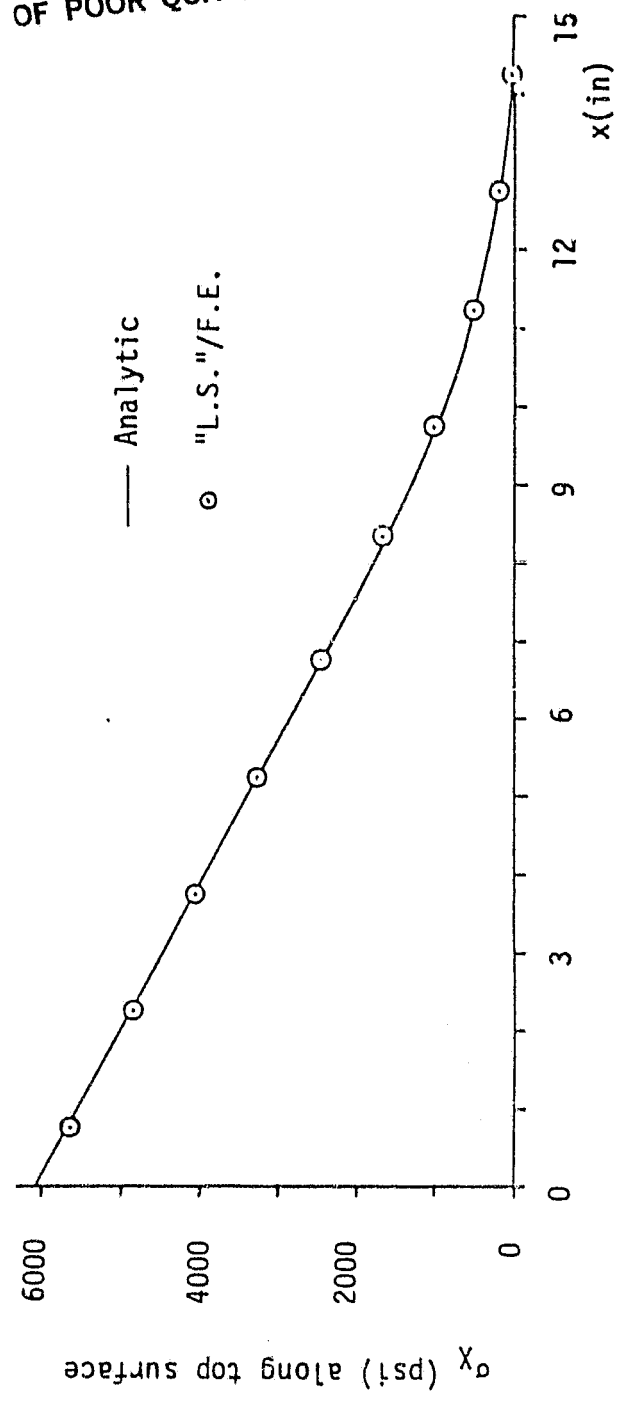

Figure 18. σ_x Along Top Surface Versus Displacements at Every Node Under Distributed Load For Cantilever Beam

ORIGINAL PAGE IS
OF POOR QUALITY

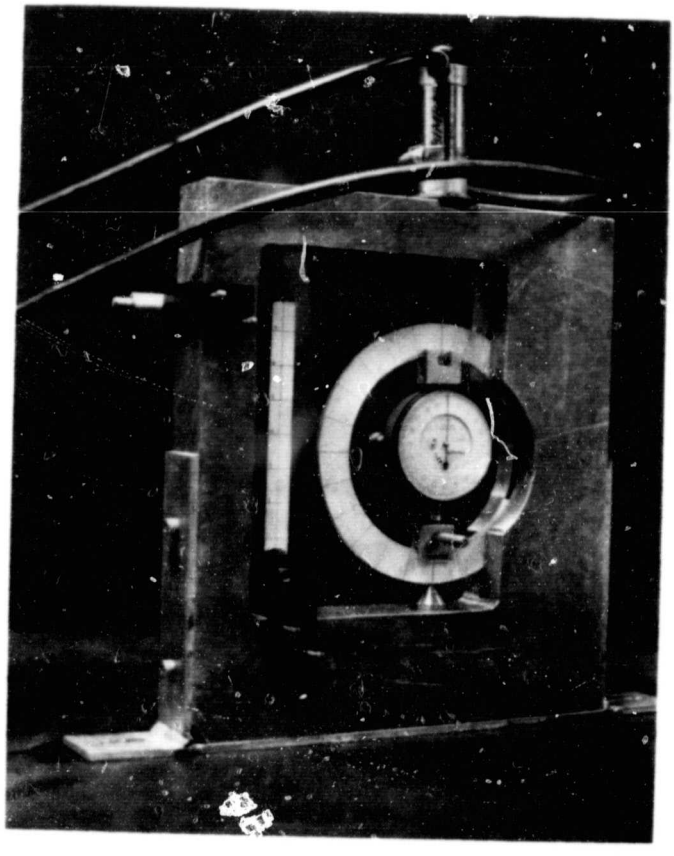

Figure 19. Load Arrangement For C-Ring

going a known rigid-body displacement would be recorded on the speckle-gram.

Speckle interferometry was used to determine the displacements which the C-ring underwent during the diametrical compression. The model was illuminated by a helium-neon laser beam diffused through a spatial filter. The images of the model were recorded on a Agfa-Gevaert 10E75 4" x 5" film plate held in a camera arrangement. The first exposure of the film plate recorded the image of the ring having a small amount of preload applied to it. The second exposure recorded the image of the ring after applying a diametrical compression which reduced the diameter along the line of action by approximately 0.01 inches (referenced to the preloaded position).

Data was taken from the specklegram along two radial lines (A-B and C-D on Fig. 20) separated by 30^{o} on the C-ring. Spacing and orientation of the Young's fringes were measured along each cross section at 13 points corresponding to the nodal points on the finite element model.

Young's fringe information was recovered from the specklegram by illuminating the film plate with an argon laser whose beam was converged with a long focal length lense. The halo was projected onto a scribed piece of frosted glass mounted such that it would be rotated to allow alignment with the fringes so that their angular orientation could be measured.

Accurate placement of the specklegram in the laser beam was accomplished by using a translating platform which could be positioned in three directions with micrometers. This platform also allowed rotation about the axis parallel to the laser beam for ease of determining a

ORIGINAL PAGE IS
OF POOR QUALITY

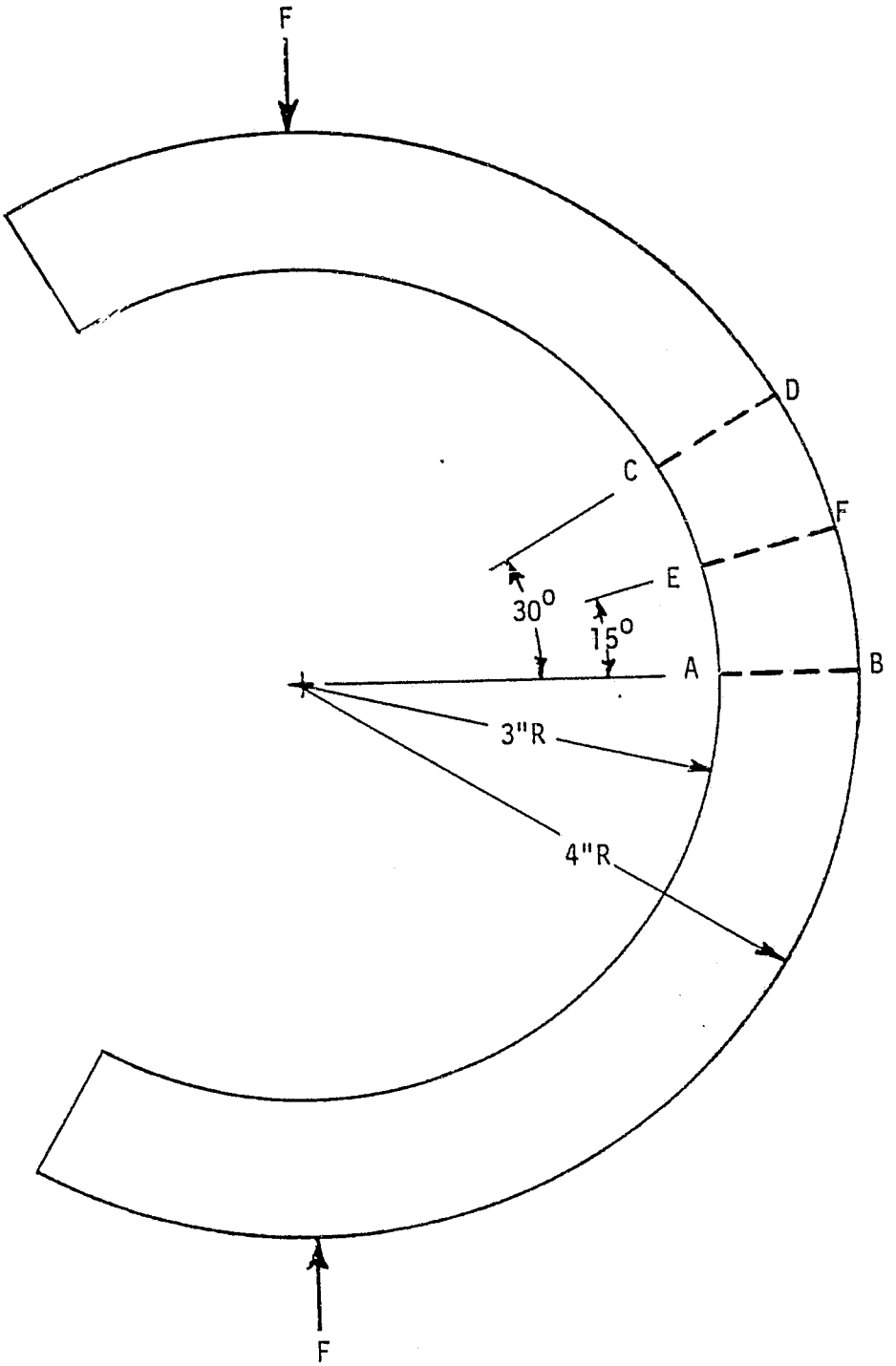

Figure 20

C-Ring in Diametrical Compression

reference orientation for the Young's fringes.

Due to symmetrical considerations, only 90 degrees of the C-ring (from the point of application of the load to the center) needed to be modeled for finite element analysis. This portion of the ring was divided into 216 elements with the density of the elements increasing toward the inside edge, (Fig. 21). The increased density of elements close to the inside edge was necessary due to greater stress gradients in this area.

To ascertain that this finite element grid would yield accurate results, the principal stresses from the finite element program were compared to those from the analytical solution. These stresses from both solutions along the cross section in the middle of the model are shown in Fig 22 . The largest difference between critical stresses of both solutions was less than 1.0% using this grid.

The Young's fringe data taken along the 0^{o} and 30^{o} lines were reduced to obtain displacements in the χ and y directions. These displacements were plotted and a "best fit" straight line was drawn through the data in order to smooth experimental error effects, (Fig.23 and 24). Data taken off of the lines were used as displacement inputs in the finite element program. These displacements defined the boundary conditions along the 0^{o} and 30^{o} lines; other boundaries (inside and outside edges) were specified as being stress free.

The validity of using a "best fit" straight line for the displacement data was investigated by plotting the analytic displacements along the 0^{o} and 30^{o} lines. A straight line drawn through this data showed very little deviation of the data from the line. Using the displacements taken from these lines as inputs, the finite element program

ORIGINAL PAGE IS
OF POOR QUALITY

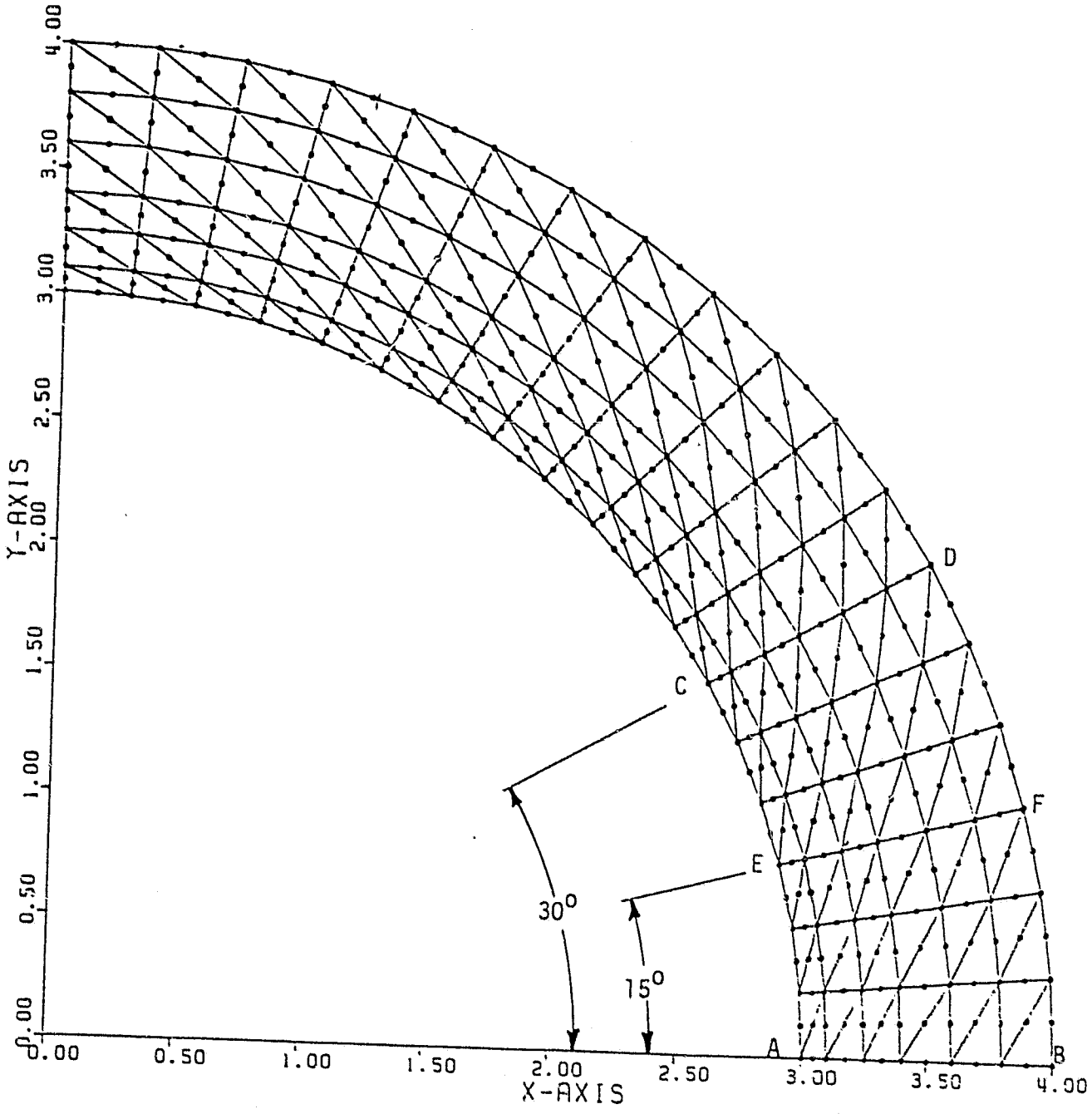

Figure 21
C-Ring Finite Elements

ORIGINAL PAGE IS
OF POOR QUALITY

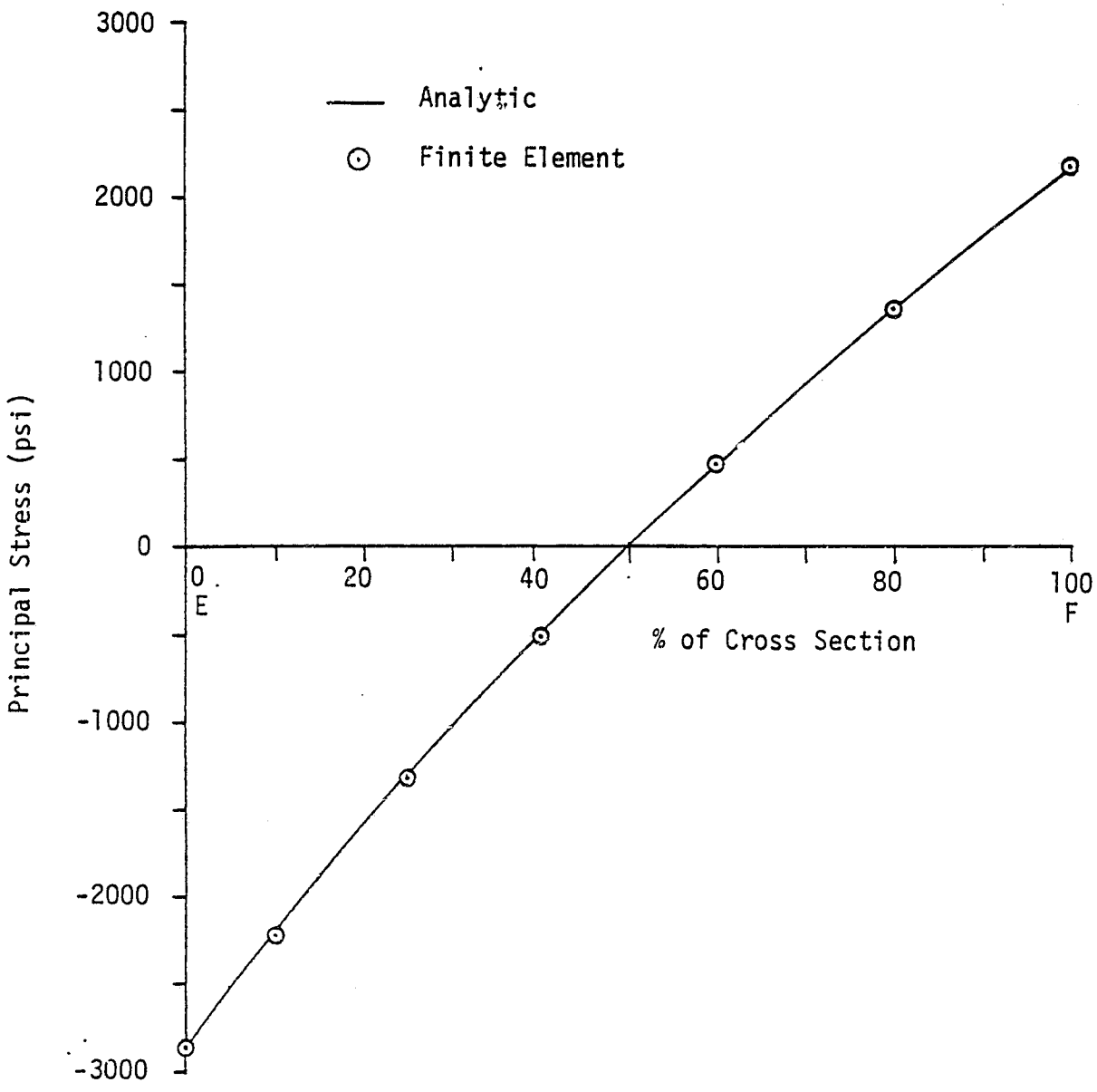

Figure 22. Principal Stress Along 15^{o} Cross Section Of C-Ring

ORIGINAL PAGE IS
OF POOR QUALITY

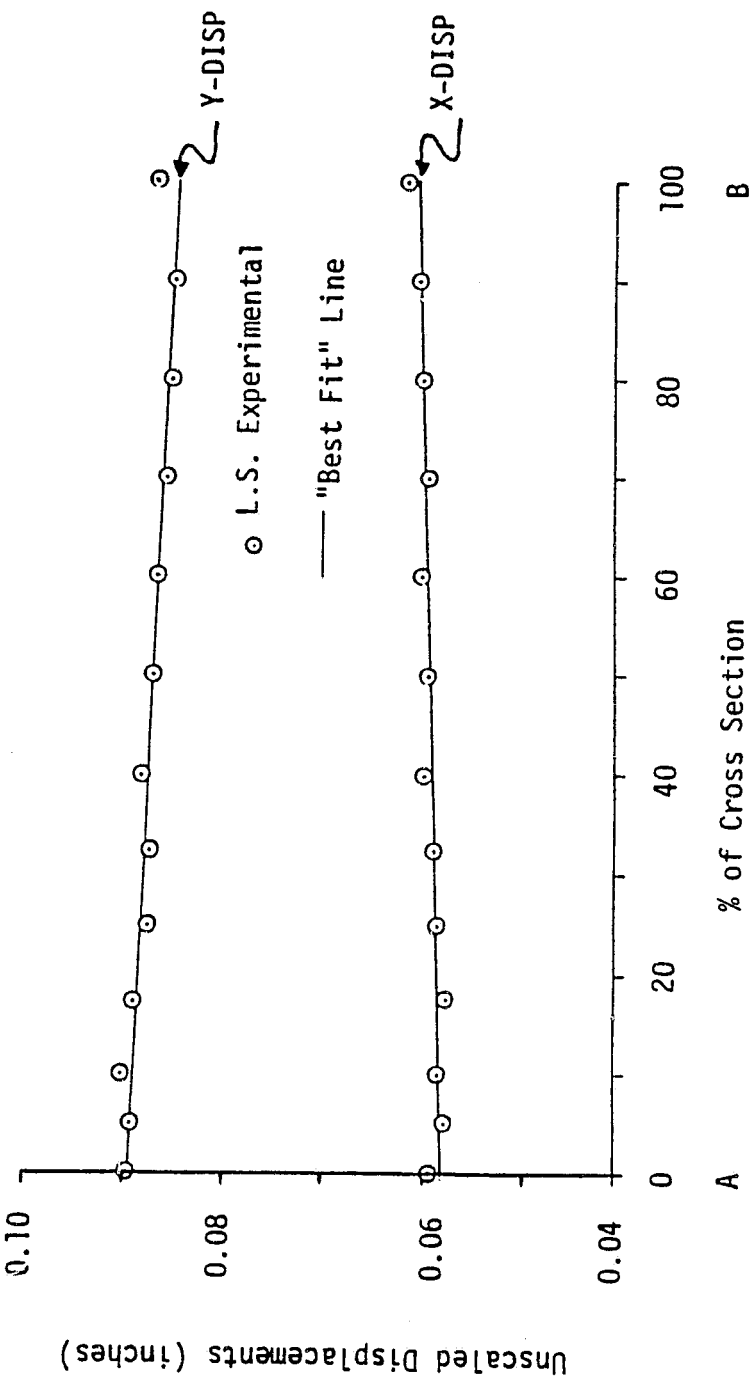

Figure 23. Displacements Along 0^0 Cross Section Of C-Ring

ORIGINAL PAGE IS
OF POOR QUALITY

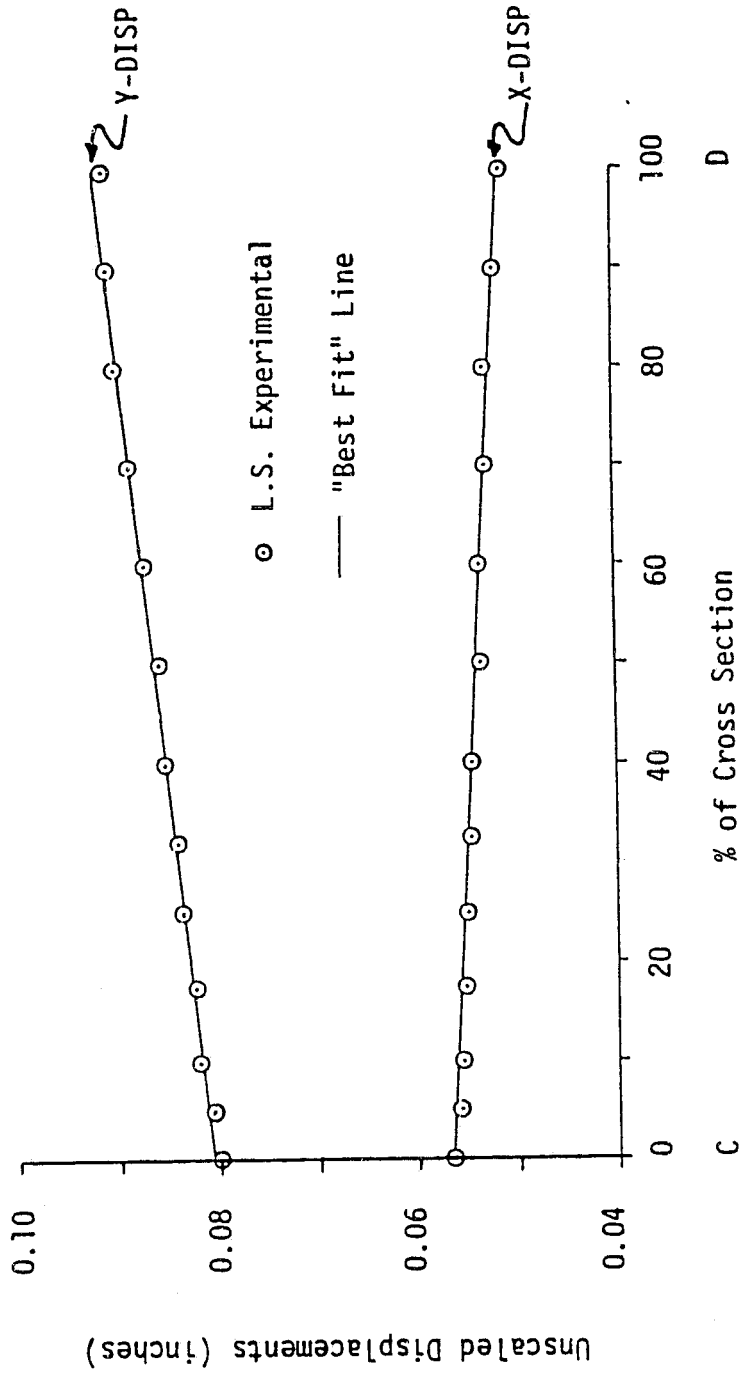

Figure 24. Displacements Along 30^{0} Cross-Section of C-Ring

determined stresses which were in very close agreement with the analytically determined stresses at points removed from the cross-sections where the displacements were input.

Principal stress results along the 15^{o} radial line from the finite element program using the straight line fit of the experimentally determined displacements is shown in Fig. 25 . It should be noted that the stresses have been scaled such that the Speckle/F.E. determined principal stress on the inside edge match the analytically determined principal stress at this point. This scaling was done because an experimental scaling factor could not be determined due to the fact that the calibration specimen appeared to have undergone other than a purely rigid body in plane displacement. This only limits comparisons of the magnitudes of the stresses and does not hinder the comparison of the trends of the stresses.

Examination of Fig.25 shows that the analytic and Speckle/F.E. principal stresses varied from the forced difference of 0 psi on the inside edge to a difference of approximately 1400 psi at the outside edge. Note that the shapes of the curves are very similar and only their placement and orientation vary significantly.

Figures 26 and 27 show new straight line fits through the experimental displacement data. Although these new straight line fits do not seem to be "best" fits, they do appear to be within the range of uncertainty for the experimental data as is indicated by the scatter of the data. When displacements from these new lines were input into the finite element program there was much better agreement between the principal stress curves as can be seen in Figure 28 . The difference between

ORIGINAL PAGE IS
OF POOR QUALITY

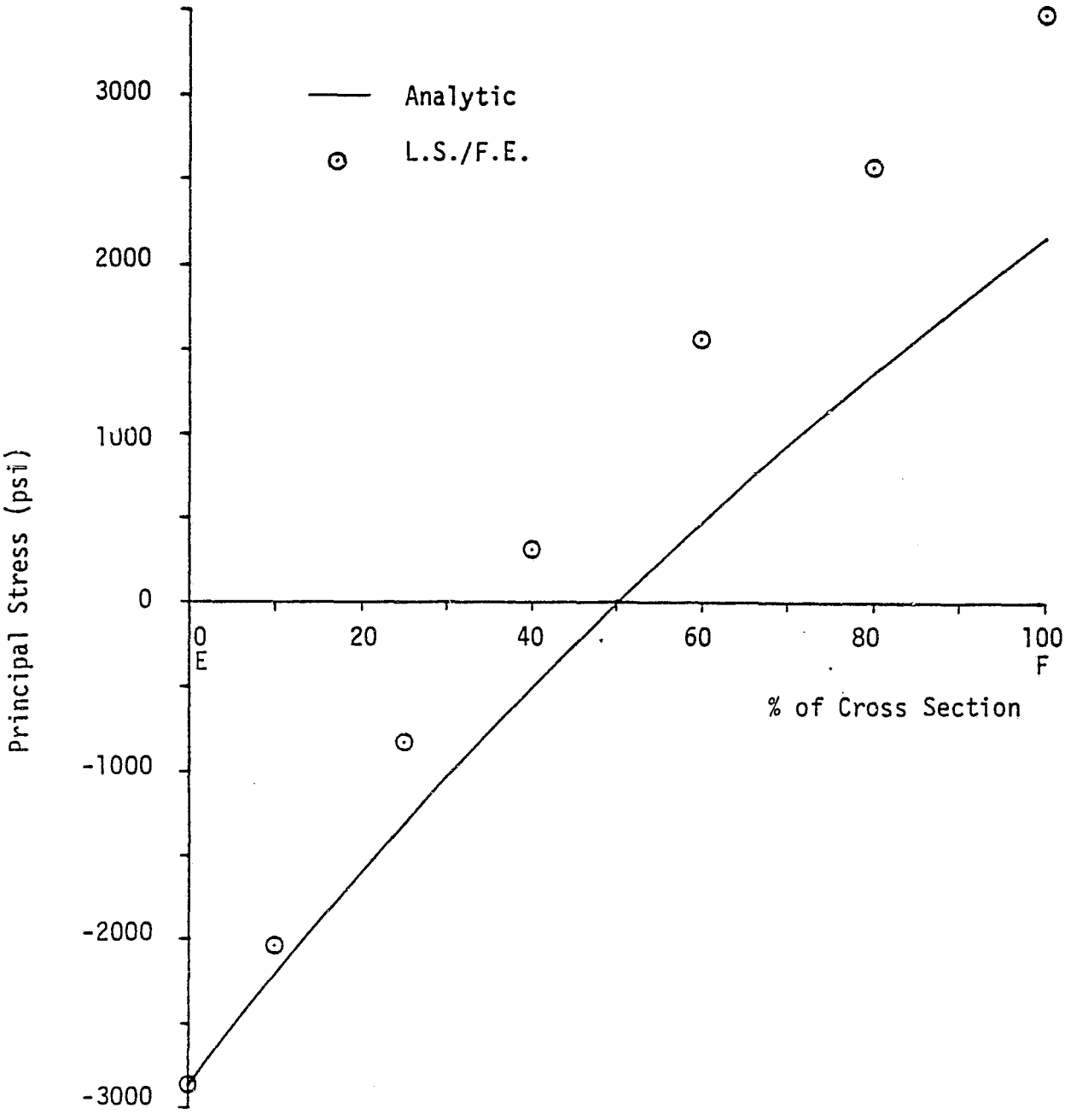

Figure 25. Principal Stress Along 15^{o} Cross Section Of C-Ring

ORIGINAL PAGE IS
OF POOR QUALITY

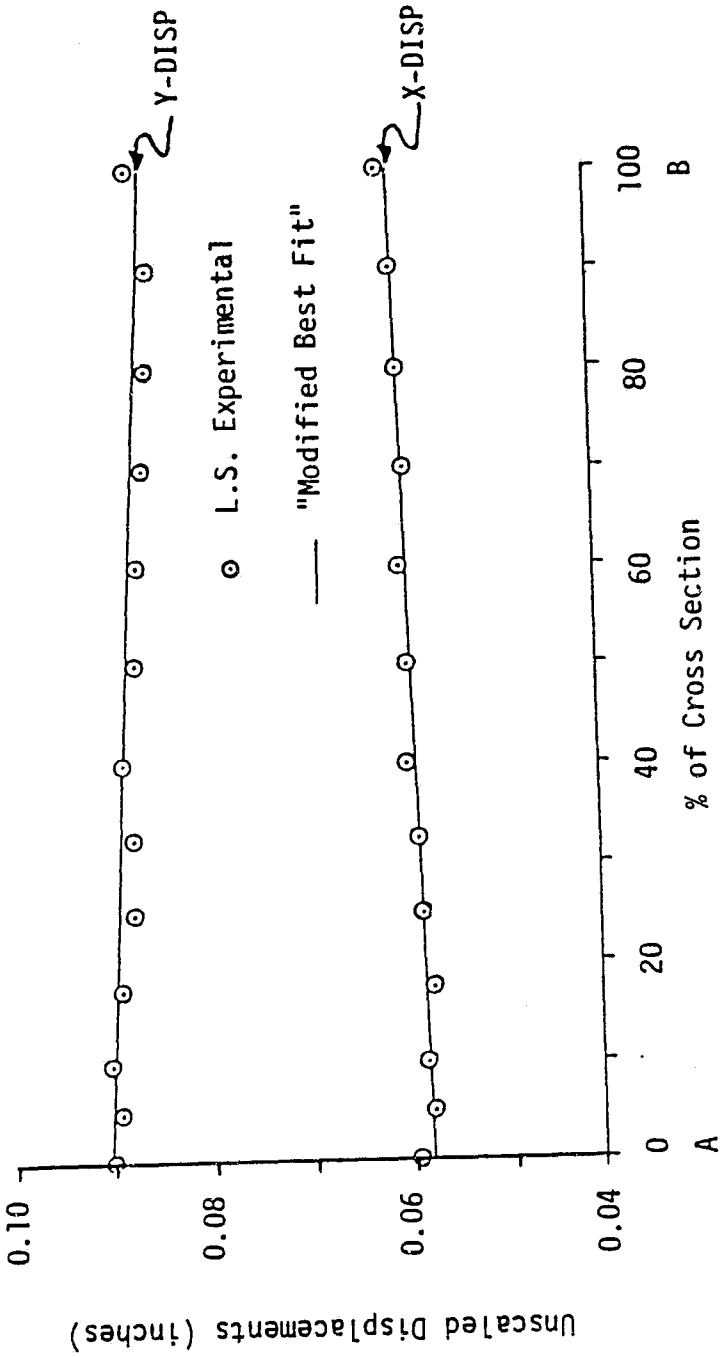

Figure 26. Displacements Along 0^{o} Cross Section of C. Ring

ORIGINAL PAGE IS
OF POOR QUALITY

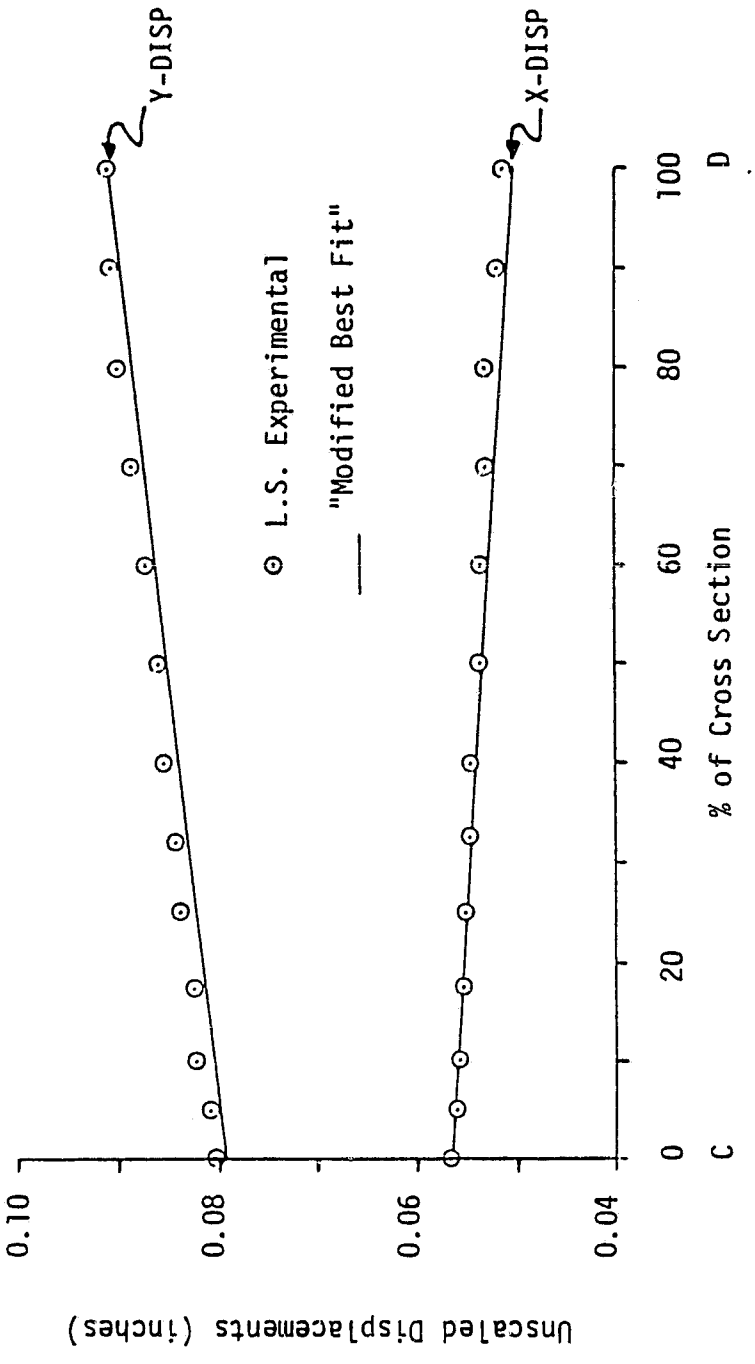

Figure 27. Displacements Along 30^{0} Cross Section of C. Ring

ORIGINAL PAGE IS
OF POOR QUALITY

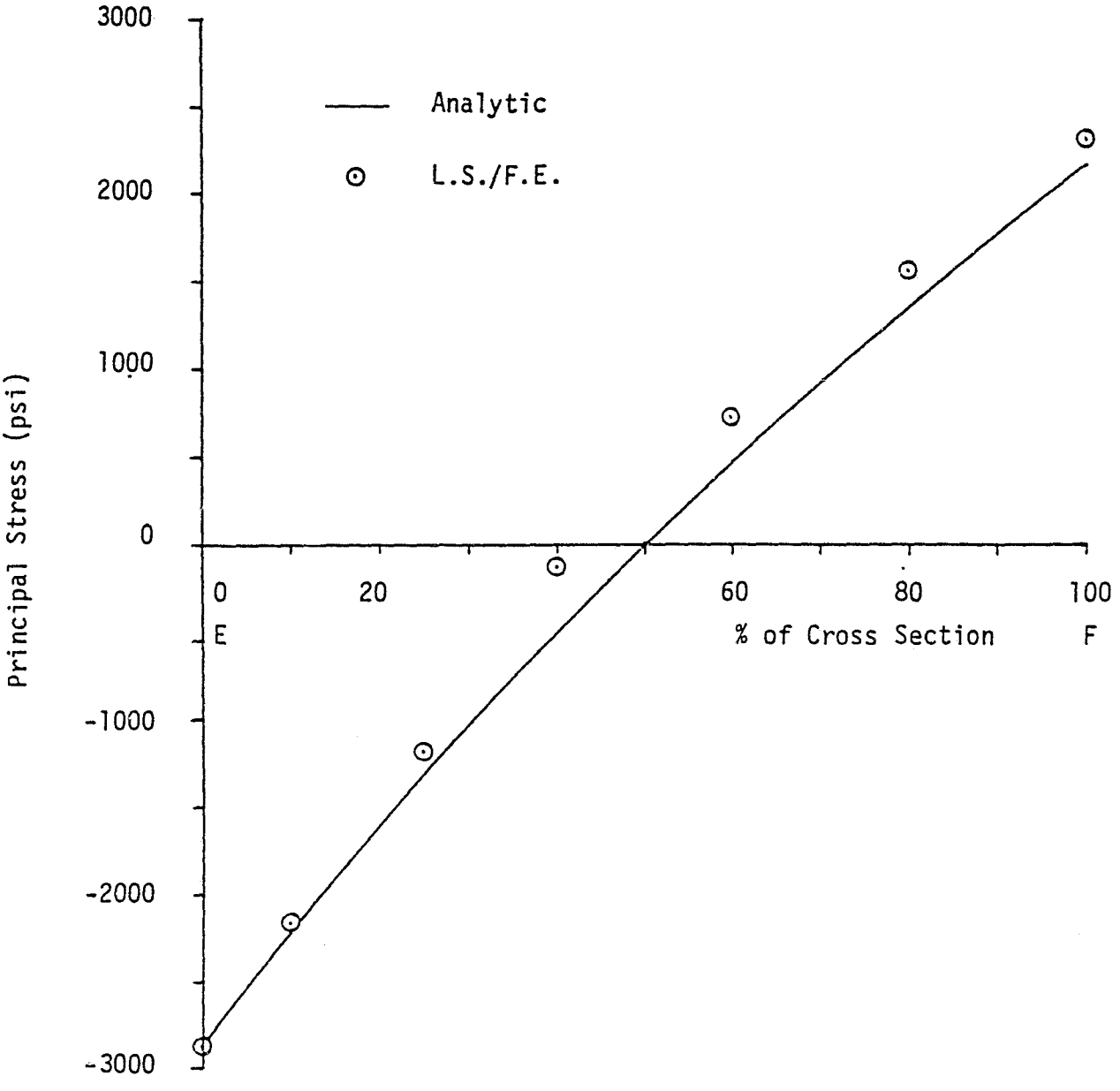

Figure 28. Principal Stress Along 15^{o} Cross Section of C. Ring

the Speckle/F.E. and the analytic principal stresses varies in this case from the forced 0 psi at the inside edge to approximately 350 psi at the middle of the cross section. Such a large variance in results for the small change in displacements input dramatizes the sensitivity of the stress results to the experimentally determined displacements.

The large scatter of experimental data about a straight line (as opposed to the straight line nature of the analytic data) indicates high uncertainty in experimental data. The fact that the Speckle/F.E. method was able to determine the general trend of the stresses from this uncertain data shows definite promise for this method. A simple numeric differentiation of displacement data would have yielded stresses not very representative of the actual stress state. However, in cases similar to the "C-ring," accurate experimental determination of displacements within a straight line approximation should allow the Speckle/F.E. method to closely determine the stress state.

REFERENCES

1. Abramson, N., "Sandwich Hologram Interferometry: A New Dimension in Holographic Comparison", Applied Optics , Vol. 13, No. 9, 1974, pp. 2019-2025.

2. Maddux, B.E. and Adams, F.D., "Development of a Dual-Plate Technique for Speckle Photography," 1976 SESA Spring Meeting, Silver Springs, Maryland, May 1976.

3. Archbold, E., Burch, J.M., and Ennos, A.E., "Recording of In-Plane Surface Displacement by Double-Exposure Speckle Photography", Optics Acta, Vol. 17, No. 12, 1970, pp. 883-898.

4. Kineriwala, V.R., Peters, W.H. Ranson, W.F. and Swinson, W.F., "Speckle Patterns for Measuring Displacements Described as Diffraction Gratings," Proceedings of 12th Annual Meeting of Society of Engineering Science held at the University of Texas at Austin, Texas, Oct. 1975, pp 413-421.

5. Sikora, J.P. and Mendenball, F.T. Jr., "Holographic Vibration Study of a Rotating Propeller Blade," Experimental Mechanics, June 1974, pp 230-232.

6. Stetson, K.A., "The use of an Image Derotator in Hologram Interferometry and Speckle Photography of Rotating Objects", Experimental Mechanics, February 1978, pp 67-73.

7. Zienkiewicz, O.C., The Finite Element Method, McGraw-Hill, 1971.

8. MacBain, J.C., "Displacement and Strain of Vibrating Structures", Experimental Mechanics, p. 361, Oct., 1978.

9. Rowlands, R.E., Segalman, D.J., Woyak, D.B., "Smooth Spline-Like Finite-Element Differentiation of Full-Field Experimental Data Over Arbitrary Geometry", Experimental Mechanics, P. 429, Dec., 1979.

10. Swinson, W.F., Turner, J.L., Ranson, W.F., "Techniques and Theories for Determining Stresses in Rotating Turbine Blades", Final Report, NASA-Lewis Research Center, Cleveland, OH, May 1980..

11. Moslehy, F.A., Ranson, W.F., "Laser Speckle and Boundary Integral Techniques in Experimental Mechanics," presented May, 1980, International Congress on Experimental Mechanics, Boston, Mass.

ORIGINAL PAGE IS
OF POOR QUALITY

Appendix

Finite Element Program

```
C*************************************************************************
C                                                                        *
C    PLNSTSGD IS A FINITE ELEMENT STRUCTURAL ANALYSIS PROGRAM WRITTEN    *
C  BY DR. JOHN L. TURNER, ASSOCIATE PROFESSOR OF AGRICULTURAL ENGINEER-  *
C  ING AT AUBURN UNIVERSITY. PLNSTSGD USES SIX NODED PLAIN STRESS TRI-   *
C  ANGULAR ELEMENTS. CONTAINED IN PLNSTSGD IS A GRID ROUTINE, DEVELOPED  *
C  BY FRANK H. VALADE, JR. AT AUBURN UNIVERSITY, WHICH GENERATES ELE-    *
C  MENTS FOR A BASIC GEOMETRY DESCRIBED BY THE USER.                     *
C                                                                        *
C*************************************************************************
C
C&&&&&&&&&&&&&&&&&&&&&&&&&&&&&&&&&&&&&&&&&&&&&&&&&&&&&&&&&&&&&&&&&&&&&&&
C  4/14/81   THIS PROGRAM HAS BEEN MODIFIED FROM THE VERSION IN STRSLIB.
C  THE CHANGES ARE SET OFF BY ROWS OF AMPERSANDS (&). JOHN WEATHERS
C&&&&&&&&&&&&&&&&&&&&&&&&&&&&&&&&&&&&&&&&&&&&&&&&&&&&&&&&&&&&&&&&&&&&&&&
C
      IMPLICIT REAL*8(A-H,O-Z)
      DIMENSION XG(481),YG(481),IMATL(216),Q(1,3,3),NOD(216,6),B(962,
     *54),F(962)
      DIMENSION STRNX(216,6),STRNY(216,6),STRNXY(216,6)
      DIMENSION STRSX(216,6),STRSY(216,6),STRSXY(216,6),TITLE(10)
      NRD=5
      NWT=6
C&&&&&&&&&&&&&&&&&&&&&&&&&&&&&&&&&&&&&&&&&&&&&&&&&&&&&&&&&&&&&&&&&&&&&&&
      READ(NRD,500) TITLE,THICK,RBDISP
  500 FORMAT(10A8,/,F10.0,F10.0)
      WRITE(NWT,600) TITLE,THICK,RBDISP
  600 FORMAT('1',10A8,/,'0','THICKNESS=',F10.4,/,'0','R.B. DISP=',F10.4)
C&&&&&&&&&&&&&&&&&&&&&&&&&&&&&&&&&&&&&&&&&&&&&&&&&&&&&&&&&&&&&&&&&&&&&&&
      READ(NRD,1)NNP,NELE,NMP,NROW,NCOL
    1 FORMAT(5I5)
      WRITE(NWT,2) NNP,NELE,NMP,NROW,NCOL
    2 FORMAT('0','NNP=',I5,/,'0','NELE=',I5,
     *       /,'0','NMP=',I5,/,'0','NROW=',I5,/,'0','NCOL=',I5)
      CALL AMAIN(NRD,NWT,NNP,NELE,NMP,NROW,NCOL,XG,YG,IMATL,Q,NOD,
     *B,F,STRNX,STRNY,STRNXY,STRSX,STRSY,STRSXY,TITLE,THICK,RBDISP)
      CALL EXIT
      STOP
      END
```

ORIGINAL PAGE IS
OF POOR QUALITY

```
      SUBROUTINE AMAIN(NRD,NWT,NNP,NELE,NMP,NROW,NCOL,XG,YG,IMATL,Q,NOD,
     *B,F,STRNX,STRNY,STRNXY,STRSX,STRSY,STRSXY,TITLE,THICK,RBDISP)
C
      IMPLICIT REAL*8(A-H,O-Z)
      DIMENSION XG(NNP),YG(NNP),IMATL(NELE),Q(NMP,3,3),NOD(NELE,6),E(3,3
     *),S(12,12),B(NROW,NCOL),F(NROW)
      DIMENSION MBCL(100),VDISP(100),STRNX(NELE,6),STRNY(NELE,6),STRNXY
     *(NELE,6),STRSX(NELE,6),STRSY(NELE,6),STRSXY(NELE,6),TITLE(10)
      LONG=100
      CALL GRID01(NNP,XG,YG,NELE,NOD)
      WRITE(NWT,17)
   17 FORMAT('1',12X,'NODE NUMBER',14X,'XG',28X,'YG')
      DO 7 I=1,NNP
C     READ(NRD,1)I,XG(I),YG(I)
    7 WRITE(NWT,16) I,XG(I),YG(I)
   16 FORMAT('0',13X,I5,15X,F10.4,20X,F10.4)
    1 FORMAT(I5,2F10.0)
C&&&&&&&&&&&&&&&&&&&&&&&&&&&&&&&&&&&&&&&&&&&&&&&&&&&&&&&&&&&&&&&&&&&&
C     READ(NRD,2)(IMATL(I),I=1,NELE)
      DO 100 I=1,NELE
  100 IMATL(I)=1
C     WRITE(NWT,19)
   19 FORMAT('1',10X)
C     WRITE(NWT,18)(I,IMATL(I),I=1,NELE)
   18 FORMAT('0','IMATL(',I3,')=',I5)
C&&&&&&&&&&&&&&&&&&&&&&&&&&&&&&&&&&&&&&&&&&&&&&&&&&&&&&&&&&&&&&&&&&&&
    2 FORMAT(50I1)
      DO 3 I=1,NMP
    3 READ(NRD,4)Q(I,1,1),Q(I,1,2),Q(I,1,3),Q(I,2,2),Q(I,2,3),Q(I,3,3)
      WRITE(NWT,19)
      WRITE(NWT,20)(((I,J,K,Q(I,J,K),K=J,3),J=1,3),I=1,NMP)
   20 FORMAT('0','Q(',I1,',',I1,',',I1,')=',E14.7)
    4 FORMAT(6E10.0)
C     DO 5 N=1,NELE
C   5 READ(NRD,6)I,(NOD(I,J),J=1,6)
    6 FORMAT(7I5)
      WRITE(NWT,21)
   21 FORMAT('1','ELEMENT NUMBER',20X,'NODE NUMBERS')
      DO 30 I=1,NELE
   30 WRITE(NWT,22) I,(NOD(I,J),J=1,6)
   22 FORMAT('0',5X,I5,10X,6(I5,5X))
      DO 10 I=1,NROW
      DO 10 J=1,NCOL
   10 B(I,J)=0.0D00
      DO 8 I=1,NELE
      N=IMATL(I)
      CALL MATL(N,Q,NMP,E)
      IF(N.EQ.18) WRITE(NWT,13) E
```

ORIGINAL PAGE IS
OF POOR QUALITY

```
      CALL STIFF(XG,YG,NOD,NELE,NNP,S,E,I,THICK)
      CALL ASSEMP(B,NROW,NCOL,S,NOD,NELE,I,12,6,2)
C     WRITE(NWT,6) I
    8 CONTINUE
C     WRITE(NWT,13)((B(I,J),J=1,NCOL),I=1,NROW)
C     WRITE(NWT,501)(F(I),I=1,NROW)
      CALL BCFORC(NBD,F,NROW)
C     WRITE(NWT,500)(F(I),I=1,NROW)
C  500 FORMAT(/,10X,6E15.4)
      CALL BCSTF3(B,F,NROW,NCOL,MBCL,VDISP,LONG,NDISP,NCOL,RBDISP)
C     WRITE(NWT,13)((B(I,J),J=1,NCOL),I=1,NROW)
C     WRITE(NWT,501)(F(I),I=1,NROW)
      CALL SYBAT(B,F,NROW,NCOL,1,NROW,NCOL)
   13 FORMAT(//,(/,6F20.6))
      WRITE (NWT,25)
   25 FORMAT('1',3X,'NODE',14X,'X-DISP.',22X,'Y-DISP.')
      DO 23 I=1,NNP
      J=2*I
      K=J-1
      WRITE(NWT,24)I,F(K),F(J)
   24 FORMAT('0',I5,15X,F14.7,15X,E14.7)
   23 CONTINUE
      WRITE(NWT,27)
   27 FORMAT('1','ELE. NO.',3X,'NODE NO.',8X,'SIGMA-X',10X,'SIGMA-Y',
     *10X,'TAU X-Y',10X,'EPSILON-X',10X,'EPSILON-Y',10X,'GAMMA X-Y')
      DO 14 I=1,NELE
      N=IMATL(I)
      CALL MATL(N,Q,NNP,E)
      CALL STRAIN(XG,YG,NOD,NELE,NNP,E,I,F,NROW,STRSX,STRSY,
     *STRSXY,STRNX,STRNY,STRNXY)
      DO 15 K=1,6
      WRITE(NWT,502)I,NOD(I,K),STRSX(I,K),STRSY(I,K),STRSXY(I,K),
     *STRNX(I,K),STRNY(I,K),STRNXY(I,K)
  502 FORMAT('0',2X,I3,6X,I4,11X,6(E14.7,3X))
C&&&&&&&&&&&&&&&&&&&&&&&&&&&&&&&&&&&&&&&&&&&&&&&&&&&&&&&&&&&&&&&&&&&&
      STSMM = DSQRT(((STRSX(I,K)-STRSY(I,K))/2.0000)**2+STRSXY(I,K)**2)
      STSMM1 = 0.5000*(STRSX(I,K)+STRSY(I,K))+STSMM
      STSMM2 = 0.5000*(STRSX(I,K)+STRSY(I,K))-STSMM
      WRITE(NWT,503) STSMM1,STSMM2
  503 FORMAT(1X,T27,2(E14.7,3X))
C&&&&&&&&&&&&&&&&&&&&&&&&&&&&&&&&&&&&&&&&&&&&&&&&&&&&&&&&&&&&&&&&&&&&
   15 CONTINUE
   14 CONTINUE
      RETURN
      END
```

ORIGINAL PAGE IS
OF POOR QUALITY

```
      SUBROUTINE ASSEMB(B,NRO ,NCO ,S,NOD,NELE,NTRI,NDIM,NNP,NDEPN)
C
C*****************************************************************************
C                                                                             *
C  THIS ROUTINE ASSEMBLES A SYMMETRIC BANDED STRUCTURAL STIFFNESS             *
C  MATRIX VIA INDIVIDUAL ELEMENTS.                                            *
C                                                                             *
C       B = GLOBAL STIFFNESS MATRIX(SYMMETRIC BANDED)                         *
C       S = ELEMENT STIFFNESS MATRIX                                          *
C       NNP = NO OF NODAL  POINTS IN ELEMENT                                  *
C       NDEPN = NO OF DEGREES OF FREEDOM PER NODE                             *
C       NDIM = DIMENSION OF ELEMENT STIFFNESS MATRIX = NNP*NDEPN              *
C       NOD = GLOBAL CONNICTIVITY VECTOR                                      *
C       NTRI = ELEMENT NO                                                     *
C       NRO = NO OF ROWS IN STRUCTURAL STIFFNESS MATRIX                       *
C       NCOL = NO OF COLUMNS IN TOTAL STRUCTURAL STIFFNESS MATRIX             *
C                                                                             *
C*****************************************************************************
C
      IMPLICIT REAL*8(A-H,O-Z)
      DIMENSION NOD(NELE,6),B(NRO ,NCO ),S(NDIM,NDIM)
C       I,IN INDEX ROWS J,JN INDEX COLUMNS
      DO 1 I=1,NNP
      NROW = (NOD(NTRI,I) - 1)*NDEPN + 1
      DO 1 J=1,NNP
      NCOL = (NOD(NTRI,J) - 1)*NDEPN + 1
C       CHECK TO SEE IF BELOW MAIN DIAGONAL
      IF(NROW.GT.NCOL) GO TO 1
      NBCOL = IABS(  NCOL-NROW)+1
C       DO ON NUMBER OF DEGREES OF FREEDOM PER NODE
      DO 2 IN=1,NDEPN
      DO 2 JN=1,NDEPN
C       CHECK FOR ELEMENTS BELOW MAIN DIAGONAL;
      IF(NBCOL.EQ.1) GO TO 10
      GO TO 11
   10 CONTINUE
      IF(JN.LT.IN) GO TO 2
   11 CONTINUE
      NBCOL1 = NBCOL+JN-IN
      NROW1 = NROW-I+IN
      NRS = NDEPN*(I-1) + IN
      NCS = NDEPN*(J-1)+JN
      B(NROW1,NBCOL1) = B(NROW1,NBCOL1) + S(NRS,NCS)
    2 CONTINUE
    1 CONTINUE
      RETURN
      END
```

ORIGINAL PAGE IS
OF POOR QUALITY

```
      SUBROUTINE BCFORC(NRD,F,NROW)
C
      IMPLICIT REAL*8(A-H,O-Z)
      DIMENSION F(NROW)
      DO 2 I=1,NROW
    2 F(I)=0.0000
      READ (NRD,1)NFORCE
      WRITE(6,3) NFORCE
    3 FORMAT('1',10X,'NFORCE=',I5)
      IF(NFORCE .EQ. 0) RETURN
      READ(NRD,1)(NVAR,F(NVAR),N=1,NFORCE)
    1 FORMAT (5(I5,E10.4))
      DO 10 I=1,NROW
      IF(F(I).EQ.0) GO TO 10
      WRITE(6,4)I,F(I)
    4 FORMAT('0','NVAR=',I5,10X,'FORCE=',E14.7)
   10 CONTINUE
      RETURN
      END
```

ORIGINAL PAGE IS
OF POOR QUALITY

```
      SUBROUTINE BCSTF3(B,F,NV,NC,MBCL,VDISP,LONG,NDISP,NBAND,RBDISP)
C
      IMPLICIT REAL*8(A-H,C-Z)
      DIMENSION B(NV,NC),F(NV,1),MBCL(LONG),VDISP(LONG)
C
C*********************************************************************
C
C  THIS ROUTINE PLACES NON ZERO DISPLACEMENTS INTO THE SYMMETRIC STIFFNRS
C
C*********************************************************************
      NRD=5
      READ(5,100) MDISP
  100 FORMAT(4I10)
      NDISP = MDISP
C NDISP = NO OF SPECIFIED DISPLACEMENTS
C THESE INCLUDE RIGID BODY DISPLACEMENTS
      READ(5,101) (VDISP(K),MBCL(K),K=1,MDISP)
C&&&&&&&&&&&&&&&&&&&&&&&&&&&&&&&&&&&&&&&&&&&&&&&&&&&&&&&&&&&&&&&&&&&&&&
C101  FORMAT(E10.4,I10)
  101 FORMAT(4(E10.7,I5))
C
C     ***** PUT IN RIGID BODY DISPLACEMENT *****
C
      DO 1001 K=1,MDISP
 1001    VDISP(K) = VDISP(K)+RBDISP
C
C&&&&&&&&&&&&&&&&&&&&&&&&&&&&&&&&&&&&&&&&&&&&&&&&&&&&&&&&&&&&&&&&&&&&&&
C MBCL = NO OF VARIABLE AT WHICH DISPLACEMENT IS SPECIFIED
CVDISP= VALUE OF DISPLACEMENT
      WRITE(6,102) MDISP
  102 FORMAT('1',10X,'NDISP=',I5)
      WRITE(6,103)(MBCL(K),VDISP(K),K=1,NDISP)
  103 FORMAT('0','NVAR=',I5,10X,'DISPL.=',E14.7)
      DO 1 I=1,NDISP
      NVAR=MBCL(I)
      VAL=VDISP(I)
      DO 2 J=1,NBAND
      NR=NVAR+1-J
      NRM = NVAR+J-1
      IF(NR-0) 3,3,4
    4 CONTINUE
      F(NR,1) = F(NR,1) -VAL*B(NR,J)
      B(NR,J) = 0.0000
    3 CONTINUE
      IF(NRM-NV) 5,5,6
    5 CONTINUE
      F(NRM,1) = F(NRM,1) - VAL*B(NVAR,J)
    6 CONTINUE
```

ORIGINAL PAGE IS
OF POOR QUALITY

```
      B(NVAR,J) = C.0000
2     CONTINUE
      B(NVAR,1) = 1.0DC0
      F(NVAR,1) = VAL
1     CONTINUE
      RETURN
      END
```

ORIGINAL PAGE IS
OF POOR QUALITY

```
      SUBROUTINE DMINV(A,N,D,L,M)
C
C     ..................................................................
C
C        SUBROUTINE DMINV
C
C        PURPOSE
C           INVERT A MATRIX (DOUBLE PRECISION VERSION)
C
C        USAGE
C           CALL DMINV(A,N,D,L,M)
C
C        DESCRIPTION OF PARAMETERS
C           A - INPUT MATRIX, DESTROYED IN COMPUTATION AND REPLACED BY
C               RESULTANT INVERSE.
C           N - ORDER OF MATRIX A
C           D - RESULTANT DETERMINANT
C           L - WORK VECTOR OF LENGTH N
C           M - WORK VECTOR OF LENGTH N
C
C        REMARKS
C           MATRIX A MUST BE A GENERAL MATRIX
C
C        SUBROUTINES AND FUNCTION SUBPROGRAMS REQUIRED
C           NONE
C
C        METHOD
C           THE STANDARD GAUSS-JORDAN METHOD IS USED. THE DETERMINANT
C           IS ALSO CALCULATED. A DETERMINANT OF ZERO INDICATES THAT
C           THE MATRIX IS SINGULAR.
C
C     ..................................................................
C
      IMPLICIT REAL*8(A-H,O-Z)
      DIMENSION A(1),L(1),M(1)
C
C        SEARCH FOR LARGEST ELEMENT
C
      D=1.0D0
      NK=-N
      DO 80 K=1,N
      NK=NK+N
      L(K)=K
      M(K)=K
      KK=NK+K
      BIGA=A(KK)
      DO 20 J=K,N
      IZ=N*(J-1)
```

ORIGINAL PAGE IS
OF POOR QUALITY

```
      DO 20 I=K,N
      IJ=IZ+I
   10 IF(DABS(BIGA)-DABS(A(IJ))) 15,20,20
   15 BIGA=A(IJ)
      L(K)=I
      M(K)=J
   20 CONTINUE
C
C        INTERCHANGE ROWS
C
      J=L(K)
      IF(J-K) 35,35,25
   25 KI=K-N
      DO 30 I=1,N
      KI=KI+N
      HOLD=-A(KI)
      JI=KI-K+J
      A(KI)=A(JI)
   30 A(JI) =HOLD
C
C        INTERCHANGE COLUMNS
C
   35 I=M(K)
      IF(I-K) 45,45,38
   38 JP=N*(I-1)
      DO 40 J=1,N
      JK=NK+J
      JI=JP+J
      HOLD=-A(JK)
      A(JK)=A(JI)
   40 A(JI) =HOLD
C
C        DIVIDE COLUMN BY MINUS PIVOT (VALUE OF PIVOT ELEMENT IS
C        CONTAINED IN BIGA)
C
   45 IF(BIGA) 48,46,48
   46 D=0.0000
      RETURN
   48 DO 55 I=1,N
      IF(I-K) 50,55,50
   50 IK=NK+I
      A(IK)=A(IK)/(-BIGA)
   55 CONTINUE
C
C        REDUCE MATRIX
C
      DO 65 I=1,N
      IK=NK+I
```

ORIGINAL PAGE IS
OF POOR QUALITY

```
      HOLD=A(IK)
      IJ=I-N
      DO 65 J=1,N
      IJ=IJ+N
      IF(I-K) 60,65,60
   60 IF(J-K) 62,65,62
   62 KJ=IJ-I+K
      A(IJ)=HOLD*A(KJ)+A(IJ)
   65 CONTINUE
C
C        DIVIDE ROW BY PIVOT
C
      KJ=K-N
      DO 75 J=1,N
      KJ=KJ+N
      IF(J-K) 70,75,70
   70 A(KJ)=A(KJ)/BIGA
   75 CONTINUE
C
C        PRODUCT OF PIVOTS
C
      D=D*BIGA
C
C        REPLACE PIVOT BY RECIPROCAL
C
      A(KK)=1.0000/BIGA
   80 CONTINUE
C
C        FINAL ROW AND COLUMN INTERCHANGE
C
      K=N
  100 K=(K-1)
      IF(K) 150,150,105
  105 I=L(K)
      IF(I-K) 120,120,108
  108 JQ=N*(K-1)
      JR=N*(I-1)
      DO 110 J=1,N
      JK=JQ+J
      HOLD=A(JK)
      JI=JR+J
      A(JK)=-A(JI)
  110 A(JI) =HOLD
  120 J=M(K)
      IF(J-K) 100,100,125
  125 KI=K-N
      DO 130 I=1,N
      KI=KI+N
```

```
      HOLD=A(KI)
      JI=KI-K+J
      A(KI)=-A(JI)
130   A(JI) =HOLD
      GO TO 100
150   RETURN
      END
```

ORIGINAL PAGE IS
OF POOR QUALITY

ORIGINAL PAGE IS
OF POOR QUALITY

```
      SUBROUTINE GRID01(L1,XG,YG,L2,NOD)
C
      IMPLICIT REAL*8(A-H,O-Z)
      DIMENSION PSPAN(20),NOD(L2,6),XG(L1),YG(L1)
      READ(5,15) NPAR
      READ(5,15) NUMS
      WRITE(6,20)NPAR,NUMS
   20 FORMAT('1',2(I5,2X))
   15 FORMAT(16I5)
      DO 1 I=1,NUMS
    1 READ(5,16) PSPAN(I)
      WRITE(6,21)(PSPAN(I),I=1,NUMS)
   21 FORMAT('0',5(F10.4,2X))
      K=1
      I1=2*NUMS+2
      DO 2 J=1,NPAR
      READ(5,16)STRX,STRY,STPX,STPY
      WRITE(6,21) STPX,STRY,STPX,STPY
   16 FORMAT(8F10.4)
      XG(K)=STRX
      YG(K)=STRY
      SPANX=STPX-STRX
      SPANY=STPY-STRY
      DO 3 L=1,NUMS
      FRAC=PSPAN(L)/100.0D0
      ENCX=SPANX*FRAC
      ENCY=SPANY*FRAC
      K1=K+1
      XG(K1)=XG(K)+ENCX/2.0000
      YG(K1)=YG(K)+ENCY/2.0000
      K2=K+2
      XG(K2)=XG(K)+ENCX
      YG(K2)=YG(K)+ENCY
    3 K=K2
    2 K=K+I1
      K=I1
      NO=I1-1
      N1=NPAR-1
      DO 4 J=1,N1
      KP=K+NO
      KM=K-NO
      XG(K)=0.5000*(XG(KM)+XG(KP))
      YG(K)=0.5000*(YG(KM)+YG(KP))
      DO 5 L=1,NUMS
      K1=K+1
      KM=KM+2
      XG(K1)=0.5000*(XG(KM)+XG(KP))
      YG(K1)=0.5000*(YG(KM)+YG(KP))
```

ORIGINAL PAGE IS
OF POOR QUALITY

```
      K2=K+2
      KP=KP+2
      XG(K2)=0.5000*(XG(KM)+XG(KP))
      YG(K2)=0.5000*(YG(KM)+YG(KP))
    5 K=K2
    4 K=K+I1
      ID=0
      I=1
      I2=I1-2
      DO 6 K=1,N1
      IA=ID*NC+1
      IB=(ID+1)*NC+1
      IC=(ID+2)*NC+1
      DO 7 J=1,NUMS
      NOD(I,1)=IA
      NOD(I,2)=IB
      NOD(I,3)=IC
      NOD(I,4)=IB+1
      NOD(I,5)=IA+2
      NOD(I,6)=IA+1
      I=I+1
      NOD(I,1)=IC
      NOD(I,2)=IC+1
      NOD(I,3)=IC+2
      NOD(I,4)=IB+2
      NOD(I,5)=IA+2
      NOD(I,6)=IB+1
      IA=IA+2
      IB=IB+2
      IC=IC+2
    7 I=I+1
    6 ID=ID+2
C       WRITE RESULTS
      L1=(NPAR*2-1)*(2*NUMS+1)
C     DO 8 N=1,L1
C   8 WRITE(6,17)N,XG(N),YG(N)
      L2=2*NUMS*(NPAR-1)
C     DO 9 N=1,L2
C   9 WRITE(6,18)(N,(NOD(N,J),J=1,6))
C  17 FORMAT('0',I5,2(3X,F10.4))
   18 FORMAT('0',7I5)
      RETURN
      END
```

ORIGINAL PAGE IS
OF POOR QUALITY

```
      SUBROUTINE MATL(A,Q,NMP,E)
C
      IMPLICIT REAL*8(A-H,O-Z)
      DIMENSION Q(NMP,3,3),Q1(3,3),E(3,3)
      DO 1 I1=1,3
      DO 1 J1=I1,3
      Q1(I1,J1)=Q(N,I1,J1)
    1 Q1(J1,I1)=Q1(I1,J1)
      DT=Q1(1,1)*(Q1(2,2)*Q1(3,3)-Q1(2,3)**2)-Q1(1,2)*(Q1(1,2)*Q1(3,3)-
     *Q1(2,3)*Q1(1,3))+Q1(1,3)*(Q1(1,2)*Q1(2,3)-Q1(2,2)*Q1(1,3))
      E(1,1)=Q1(2,2)*Q1(3,3)-Q1(2,3)**2
      E(1,2)=-Q1(1,2)*Q1(3,3)+Q1(1,3)*Q1(2,3)
      E(1,3)=Q1(1,2)*Q1(2,3)-Q1(2,2)*Q1(1,3)
      E(2,2)=Q1(1,1)*Q1(3,3)-Q1(1,3)**2
      E(2,3)=-Q1(1,1)*Q1(2,3)+Q1(1,2)*Q1(1,3)
      E(3,3)=Q1(1,1)*Q1(2,2)-Q1(1,2)**2
      DO 3 J1=1,3
      DO 3 K1=J1,3
      E(J1,K1)=E(J1,K1)/DT
      E(K1,J1)=E(J1,K1)
    3 CONTINUE
      RETURN
      END
```

ORIGINAL PAGE IS
OF POOR QUALITY

```
      SUBROUTINE STIFF(XG,YG,NOD,NELE,NNP,S,E,IE,THICK)

      IMPLICIT REAL*8(A-H,O-Z)
      DIMENSION XG(NNP),YG(NNP),NOD(NELE,6),S(12,12),
     *C(3,3),X(6),Y(6),C(6,6)
      DIMENSION XXINT(6,6),YYINT(6,6),XYINT(6,6)
      DIMENSION IT1(6),IT2(6)
      KN1=NOD(IE,1)
      KN2=NOD(IE,2)
      KN3=NOD(IE,3)
      KN4=NOD(IE,4)
      KN5=NOD(IE,5)
      KN6=NOD(IE,6)
      X(1)=XG(KN1)
      X(2)=XG(KN2)
      X(3)=XG(KN3)
      X(4)=XG(KN4)
      X(5)=XG(KN5)
      X(6)=XG(KN6)
      Y(1)=YG(KN1)
      Y(2)=YG(KN2)
      Y(3)=YG(KN3)
      Y(4)=YG(KN4)
      Y(5)=YG(KN5)
      Y(6)=YG(KN6)
      DO 1 I=1,6
      C(I,1)=1.0D00
      C(I,2)=X(I)
      C(I,3)=Y(I)
      C(I,4)=X(I)*Y(I)
      C(I,5)=X(I)*X(I)
    1 C(I,6)=Y(I)*Y(I)
      CALL DMINV(C,6,D,IT1,IT2)
      XC=(X(1)+X(3)+X(5))/3.0D00
      YC=(Y(1)+Y(3)+Y(5))/3.0D00
      DO 2 I=1,6
      X(I)=X(I)-XC
    2 Y(I)=Y(I)-YC
      AA=0.5000*(X(1)*(Y(3)-Y(5))+X(3)*(Y(5)-Y(1))+
     *X(5)*(Y(1)-Y(3)))
      A=DABS(AA)
      P1=XC*YC+(1.0D00/12.0D00)*(X(1)*Y(1)+X(3)*Y(3)+X(5)*Y(5))
      P2=YC*YC+(1.0D00/12.0D00)*(Y(1)*Y(1)+Y(3)*Y(3)+Y(5)*Y(5))
      P3=XC*XC+(1.0D00/12.0D00)*(X(1)*X(1)+X(3)*X(3)+X(5)*X(5))
      DO 3 I=1,6
      DO 3 J=I,6
      XXINT(I,J)=A*(C(2,I)*C(2,J)+2.0D00*XC*(C(2,I)*C(5,J)+C(5,I)*
     *C(2,J))+YC*(C(4,I)*C(2,J)+C(2,I)*C(4,J))+2.0D00*P1*(C(5,I)*
```

ORIGINAL PAGE IS
OF POOR QUALITY

```
     *C(4,J)+C(4,I)*C(5,J))+C(4,I)*C(4,J)*P2+4.0D00*C(5,I)*C(5,J)*P3)
    3 YYINT(I,J)=A*(C(2,I)*C(3,J)+2.0DC0*YC*(C(3,I)*C(6,J)+C(6,I)*
     *C(3,J))+XC*(C(3,I)*C(4,J)+C(4,I)*C(3,J))+2.0D00*P1*(C(4,I)*C(6,J)+
     *C(6,I)*C(4,J))+C(4,I)*C(4,J)*P3+4.0D00*C(6,I)*C(6,J)*P2)
      DO 4 I=1,5
      K=I+1
      DO 4 J=K,6
      XXINT(J,I)=XXINT(I,J)
    4 YYINT(J,I)=YYINT(I,J)
      DO 5 I=1,6
      DO 5 J=1,6
    5 XYINT(I,J)=A*(C(2,I)*C(3,J)+XC*(C(2,I)*C(4,J)+2.0D00*C(5,I)*
     *C(3,J))+YC*(2.0D00*C(2,I)*C(6,J)+C(4,I)*C(3,J))+(C(4,I)*C(4,J)+
     *C(5,I)*C(6,J)*4.0D00)*P1+2.0DC0*C(4,I)*C(6,J)*P2+2.0D00*C(5,I)*
     *C(4,J)*P3)
      J=1
      DO 10 N=1,6
      S(1,J)=E(1,1)*XXINT(1,N)+E(1,3)*(XYINT(1,N)+XYINT(N,1))+E(3,3)*
     *YYINT(1,N)
      J=J+1
      S(1,J)=E(1,2)*XYINT(1,N)+E(1,3)*XXINT(1,N)+E(3,2)*YYINT(1,N)+E(3,3
     *)*XYINT(N,1)
      S(2,J)=E(2,2)*YYINT(1,N)+E(2,3)*(XYINT(N,1)+XYINT(1,N))+E(3,3)*
     *XXINT(1,N)
   10 J=J+1
      J=3
      DO 20 N=2,6
      S(2,J)=E(2,1)*XYINT(N,1)+E(2,3)*YYINT(1,N)+E(3,1)*XXINT(1,N)+
     *E(3,3)*XYINT(1,N)
      S(3,J)=E(1,1)*XXINT(2,N)+E(1,3)*(XYINT(2,N)+XYINT(N,2))+E(3,3)*
     *YYINT(2,N)
      J=J+1
      S(3,J)=E(1,2)*XYINT(2,N)+E(1,3)*XXINT(2,N)+E(2,3)*YYINT(2,N)+
     *E(3,3)*XYINT(N,2)
      S(4,J)=E(2,2)*YYINT(2,N)+E(2,3)*(XYINT(N,2)+XYINT(2,N))+E(3,3)*
     *XXINT(2,N)
   20 J=J+1
      J=5
      DO 30 N=3,6
      S(4,J)=E(2,1)*XYINT(N,2)+E(2,3)*YYINT(2,N)+E(3,1)*XXINT(2,N)+
     *E(3,3)*XYINT(2,N)
      S(5,J)=E(1,1)*XXINT(3,N)+E(1,3)*(XYINT(3,N)+XYINT(N,3))+
     *E(3,3)*YYINT(3,N)
      J=J+1
      S(5,J)=E(1,2)*XYINT(3,N)+E(1,3)*XXINT(3,N)+E(3,2)*YYINT(3,N)+
     *E(3,3)*XYINT(N,3)
      S(6,J)=E(2,2)*YYINT(3,N)+E(2,3)*(XYINT(N,3)+XYINT(3,N))+
     *E(3,3)*XXINT(3,N)
```

ORIGINAL PAGE IS
OF POOR QUALITY

```
30 J=J+1
   J=7
   DO 40 N=4,6
   S(6,J)=E(2,1)*XYINT(N,3)+E(2,3)*YYINT(3,N)+E(3,1)*XXINT(3,N)+
  *E(3,3)*XYINT(3,N)
   S(7,J)=E(1,1)*XXINT(4,N)+E(1,3)*(XYINT(4,N)+XYINT(N,4))+
  *E(3,3)*YYINT(4,N)
   J=J+1
   S(7,J)=E(1,2)*XYINT(4,N)+E(1,3)*XXINT(4,N)+E(3,2)*YYINT(4,N)+
  *E(3,3)*XYINT(N,4)
   S(8,J)=E(2,2)*YYINT(4,N)+E(2,3)*(XYINT(N,4)+XYINT(4,N))+
  *E(3,3)*XXINT(4,N)
40 J=J+1
   J=9
   DO 50 N=5,6
   S(8,J)=E(2,1)*XYINT(N,4)+E(2,3)*YYINT(4,N)+E(3,1)*XXINT(4,N)+
  *E(3,3)*XYINT(4,N)
   S(9,J)=E(1,1)*XXINT(5,N)+E(1,3)*(XYINT(5,N)+XYINT(N,5))+
  *E(3,3)*YYINT(5,N)
   J=J+1
   S(9,J)=E(1,2)*XYINT(5,N)+E(1,3)*XXINT(5,N)+E(3,2)*YYINT(5,N)+
  *E(3,3)*XYINT(N,5)
   S(10,J)=E(2,2)*YYINT(5,N)+E(2,3)*(XYINT(N,5)+XYINT(5,N))+
  *E(3,3)*XXINT(5,N)
50 J=J+1
   S(10,11)=E(2,1)*XYINT(6,5)+E(2,3)*YYINT(5,6)+E(3,1)*XXINT(5,6)+
  *E(3,3)*XYINT(5,6)
   S(11,11)=E(1,1)*XXINT(6,6)+E(1,3)*(XYINT(6,6))*2.0D00+E(3,3)*
  *YYINT(6,6)
   S(11,12)=E(1,2)*XYINT(6,6)+E(1,3)*XXINT(6,6)+E(2,3)*YYINT
  *(6,6)+E(3,3)*XYINT(6,6)
   S(12,12)=E(2,2)*YYINT(6,6)+E(2,3)*(XYINT(6,6))*2.0D00+E(3,3)*
  *XXINT(6,6)
   DO 60 I=1,11
   K=I+1
   DO 60 J=K,12
   S(J,I)=S(I,J)
60 CONTINUE
C&&&&&&&&&&&&&&&&&&&&&&&&&&&&&&&&&&&&&&&&&&&&&&&&&&&&&&&&&&&&&&&&&&&&&&&&&&&&
   DO 70 I=1,12
     DO 70 J=1,12
       S(I,J)=S(I,J)*THICK
70 CONTINUE
C&&&&&&&&&&&&&&&&&&&&&&&&&&&&&&&&&&&&&&&&&&&&&&&&&&&&&&&&&&&&&&&&&&&&&&&&&&&&
   RETURN
   END
```

ORIGINAL PAGE IS
OF POOR QUALITY

```
      SUBROUTINE STRAIN(XG,YG,NOD,NELE,NNP,E,IE,F,NROW,STRSX,STRSY,STRS
     *XY,STRNX,STRNY,STRNXY)
C
      IMPLICIT REAL*8(A-H,O-Z)
      DIMENSION XG(NNP),YG(NNP),NOD(NELE,6),E(3,3),F(NROW),C(6,6)
      DIMENSION STRSX(NELE,6),STRSY(NELE,6),STRSXY(NELE,6),STRNX(NELE,6)
     *,STRNY(NELE,6),STRNXY(NELE,6)
      DIMENSION X(6),Y(6),IT1(6),IT2(6)
      KN1=NOD(IE,1)
      KN2=NOD(IE,2)
      KN3=NOD(IE,3)
      KN4=NOD(IE,4)
      KN5=NOD(IE,5)
      KN6=NOD(IE,6)
C     ESTABLISH C MATRIX
      X(1)=XG(KN1)
      X(2)=XG(KN2)
      X(3)=XG(KN3)
      X(4)=XG(KN4)
      X(5)=XG(KN5)
      X(6)=XG(KN6)
      Y(1)=YG(KN1)
      Y(2)=YG(KN2)
      Y(3)=YG(KN3)
      Y(4)=YG(KN4)
      Y(5)=YG(KN5)
      Y(6)=YG(KN6)
C     COMPUTE C MATRIX
      DO 1 I=1,6
      C(I,1)=1.0000
      C(I,2)=X(I)
      C(I,3)=Y(I)
      C(I,4)=X(I)*Y(I)
      C(I,5)=X(I)*X(I)
    1 C(I,6)=Y(I)*Y(I)
C     INVERT C MATRIX AND OVERWRITE
      CALL DMINV(C,6,D,IT1,IT2)
C     COMPUTE STRAINS AT NODES
      DO 25 N=1,6
      STRNX(IE,N)=0.0000
      STRNY(IE,N)=0.0000
      STRNXY(IE,N)=0.0000
      DO 25 J=1,6
      NN=NOD(IE,J)
      JU=2*NN-1
      JV=JU+1
      STRNX(IE,N)=STRNX(IE,N)+(C(2,J)+Y(N)*C(4,J)+
     *2.0000*X(N)*C(5,J))*F(JU)
```

ORIGINAL PAGE IS
OF POOR QUALITY

```
      STRNY(IE,N)=STRNY(IE,N)+(C(3,J)+X(N)*C(4,J)+
     *2.0DC0*Y(N)*C(6,J))*F(JV)
   25 STRNXY(IE,N)=STRNXY(IE,N)+(C(3,J)+X(N)*C(4,J)+2.0D00*Y(N)*
     *C(6,J))*F(JV1)+(C(2,J)+Y(N)*C(4,J)+2.0DC0*X(N)*C(5,J))*F(JV)
      COMPUTE STRESSES
      DO 26 N=1,6
      STRSX(IE,N)=E(1,1)*STRNX(IE,N)+E(1,2)*STRNY(IE,N)+E(1,3)*STRNXY(
     *IE,N)
      STRSY(IE,N)=E(1,2)*STRNX(IE,N)+E(2,2)*STRNY(IE,N)+E(2,3)
     **STRNXY(IE,N)
   26 STRSXY(IE,N)=E(1,3)*STRNX(IE,N)+E(2,3)*STRNY(IE,N)+
     *E(3,3)*STRNXY(IE,N)
      RETURN
      END
```

ORIGINAL PAGE IS
OF POOR QUALITY

```
      SUBROUTINE SYMAT(A,B,NROW,NCOL ,ISIG,NV,NC)
C
C   THIS SUBROUTINE SOLVES SYSTEMS OF SIMULTANEOUS LINEAR EQ-
C   UATIONS FOR WHICH THE MATRIX OF COEFFICIENTS (CALLED A)
C   IS BOTH SYMMETRIC AND BANDED.  THE MATRIX A IS DIMENSION-
C   ED A(NROW,NCOL) WHERE NROW IS THE NUMBER OF EQUATIONS AND
C   NCOL IS THE BAND WIDTH.  THE PRINCIPAL DIAGONAL IS STORED
C   IN THE FIRST COLUMN OF A AND THE NONZERO BANDS ABOVE THE
C   PRINCIPAL DIAGONAL FORM THE BALANCE OF A.  THE RIGHT HAND
C   SIDE COLUMN VECTORS ARE STORED IN B WITH EACH RIGHT HAND
C   SIDE FORMING ONE COLUMN.  HENCE B IS DIMENSIONED B(NROW,
C   NRHS) WHERE NRHS IS THE NUMBER OF RIGHT HAND SIDES FOR
C   WHICH THE SOLUTION IS DESIRED.  KO IS AN EXECUTION INDIC-
C   ATOR.  IF,UPON RETURN TO THE CALLING PROGRAM, KC IS ZERO,
C   THE EXECUTION WAS SUCCESSFUL AND THE ANSWERS ARE STORED
C   IN B.  IF KC IS NOT ZERO, THE EXECUTION FAILED BECAUSE
C   THE PRINCIPAL DIAGONAL ELEMENT IN THE KC'TH ROW WAS ZERO.
C   IN THIS EVENT A NOTE IS WRITTEN ON THE OUTPUT PAGE.  THIS
C   ROUTINE DESTROYS THE MATRICES A AND B.
C
      IMPLICIT REAL*8(A-H,O-Z)
      DIMENSION A(NV,NC),B(NV,1)
C NV,NC = ABSOLUTE DIMENSIONS OF A,B NROW = NO OF VARIABLES IN MATRIX
C NCOL = BANDWIDTH OF PRESENT SET OF EQUATIONS
C ISIG = 2 SIGNALS ONLY REDUCTION OF R.H.S.VECTOR AND BACK SUBSTITUTION
  101 FORMAT(//64H YOU GOOFED --- THERE IS A ZERO ON THE PRINCIPAL DIAGO
     1NAL IN THE,I4,3H TH ROW.//)
      GO TO(18,19), ISIG
   18 CONTINUE
      NHALF=NCOL-1
      NROWM=NROW-1
      NROWH=NROW-NHALF
      DO 6 I=1,NROWM
      IF(A(I,1)) 1,15,1
    1 RECIP=1.0D00/A(I,1)
      IF(I-NROWH) 2,2,3
    2 LIMIT=NHALF
      GO TO 4
    3 LIMIT=NROW-I
    4 DO 6 J=1,LIMIT
      JROW=I+J
      RATIO=-A(I,J+1)*RECIP
      DO 5 K=J,LIMIT
      JCOL=K+1-J
    5 A(JROW,JCOL)=A(JROW,JCOL)+RATIO*A(I,K+1)
    6 CONTINUE
   19 CONTINUE
C
```

ORIGINAL PAGE IS
OF POOR QUALITY

```
      DO 17 I=1,NROWM
      DO 17 J=1,NHALF
      IJ = I+J
      IF(IJ.GT.NROW) GO TO 17
      B(IJ,1) = B(IJ,1) - B(I,1)*A(I,J+1)/A(I,1)
17    CONTINUE
C
      IF(A(NROW,1)) 7,14,7
    7 RECIP=1.CD00/A(NROW,1)
    8 B(NROW,1)=B(NROW,1)*RECIP
      DO 13 I=1,NROWM
      IROW=NROW-I
      RECIP=1.0000/A(IROW,1)
      IF(I-NHALF) 9,10,10
    9 LIMIT=I
      GO TO 11
   10 LIMIT=NHALF
   11 DO 12 J=1,LIMIT
      JROW=IROW+J
      JCOL=J+1
   12 B(IROW,1)=B(IROW,1)-A(IROW,JCOL)*B(JROW,1)
   13 B(IROW,1)=B(IROW,1)*RECIP
      KO=0
      RETURN
   14 I=NROW
   15 KC=I
      WRITE(6,101)KO
      RETURN
      END
```